Chapter 2
Equations of Motion of a Rigid Spherical Body

In this chapter, we introduce basic equations of dynamics of a rigid body during motion about a fixed pivot point. On the basis of these equations, later in this work, we will describe gyroscopic phenomena.

2.1 Kinematics of Rigid-Body Motion

To describe the spherical motion of a rigid body, it is necessary to find angular coordinates that uniquely determine the position of a rigid body in the reference frame [1–3]. In what follows, we take two frames (Fig. 2.1).

The first frame, $OX'_{1O}X'_{2O}X'_{3O}$, is a reference frame. In the considered problem, we can think of it as a fixed coordinate system. The second frame, $OX'''_1X'''_2X'''_3$, is stiff-connected with the body so that it rotates. The origins O of both these frames are the same fixed point. The position of a body with respect to the fixed coordinate system $OX'_{1O}X'_{2O}X'_{3O}$ is described by means of three angles of rotation. This means that a rotation of the body about an arbitrarily oriented axis in space, originating from point O, can be composed of another three rotations. The angles of these rotations can be specified in various ways. There exist many ways of describing the same position of a body by means of three angles [1–3]. The most popular technique was proposed by Euler.

2.1.1 The Euler Angles

After Euler,the position of a fixed-body frame $OX_1X_2X_3$ relative to the fixed frame $OX'_{1O}X'_{2O}X'_{3O}$ can be specified by the three angles Ψ_e, ϑ_e, Φ_e depicted in Fig. 2.2.

J. Awrejcewicz and Z. Koruba, *Classical Mechanics*, Advances in Mechanics and Mathematics 30, DOI 10.1007/978-1-4614-3978-3_2,

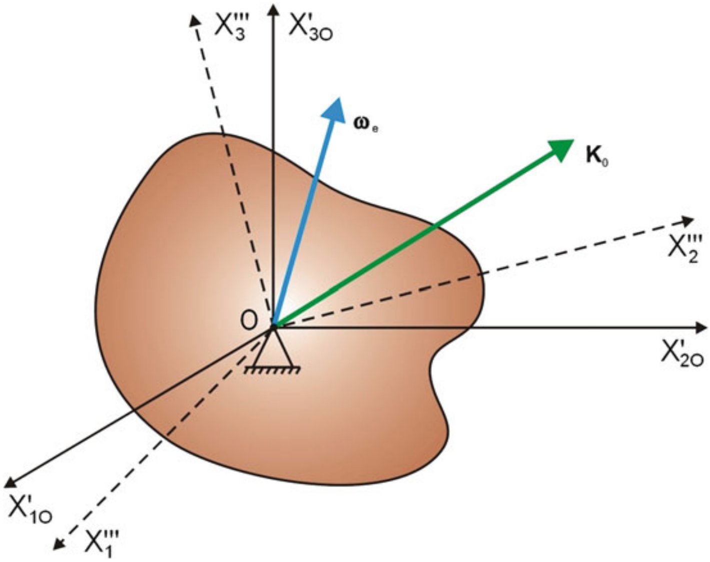

Fig. 2.1 Position of body in frames

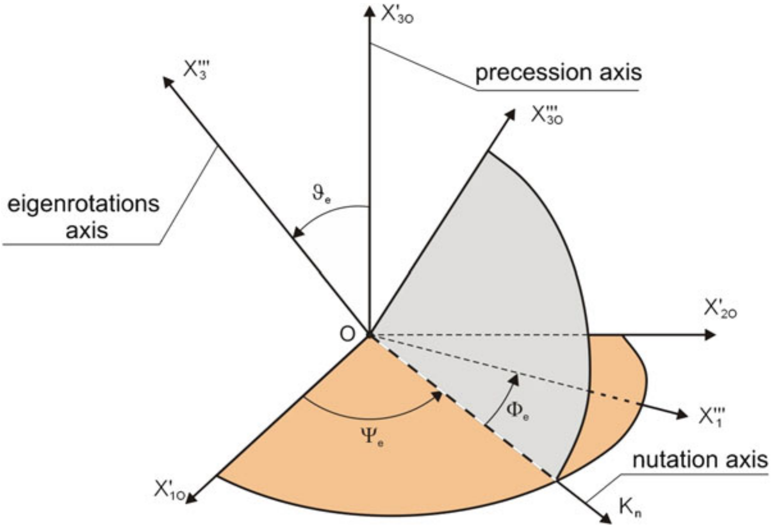

Fig. 2.2 Euler's angles

The angle ϑ_e is between two axes OX'_{3O} and OX_3. The two remaining angles are measured in the planes $OX'_{1O}X'_{2O}$ and $OX'''_1X'''_2$ (Fig. 2.2). Following the description given in [1–3], a line of intersection of these planes is called a *line of nodes* (K_n) or *axis of nutation*. The angle ψ_e is between a line of nodes and

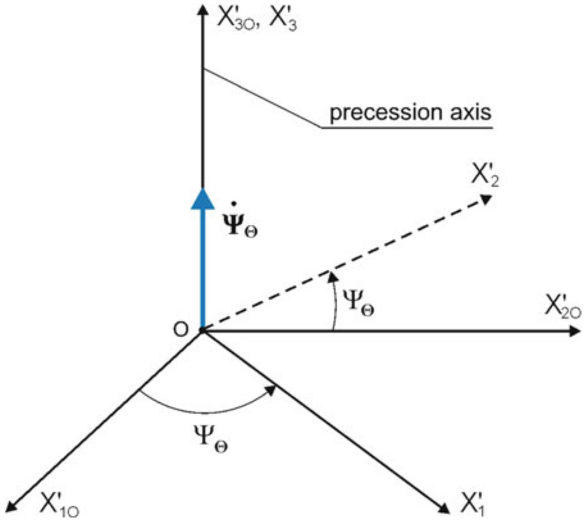

Fig. 2.3 Rotation about precession axis

the axis OX'_{1O}, and the angle Φ_e is between the line of nodes and the axis OX_1'''. In the theory of gyroscopes, angles ϑ_e, ψ_e, and ϕ_e are called *nutation*, *precession*, and *eigenrotations*, respectively. However, it should be emphasized that these terms are geometrical names and should not be confused with notions of nutation and precession, used in the rest of this work with a completely different meaning.

Thus, in the Euler approach an arbitrary position of a body can be specified as follows:

1. The first rotation is made about the OX_3''' axis by a precession angle ψ_e (Fig. 2.3).

   This orthogonal transformation can be presented by means of a matrix of transformation:

$$m^{\psi} = \begin{bmatrix} \cos\psi_e & \sin\psi_e & 0 \\ -\sin\psi_e & \cos\psi_e & 0 \\ 0 & 0 & 1 \end{bmatrix}.$$

2. The second rotation is made about the OX_1' axis by a nutation angle ϑ_e (Fig. 2.4).

   This operation is equivalent to the matrix

$$m^{\vartheta} = \begin{bmatrix} 1 & 0 & 0 \\ 0 & \cos\vartheta_e & \sin\vartheta_e \\ 0 & -\sin\vartheta_e & \cos\vartheta_e \end{bmatrix}.$$

3. The final rotation needs to be made about the axis of eigenrotations OX_3'' by an angle ϕ_e (Fig. 2.5).

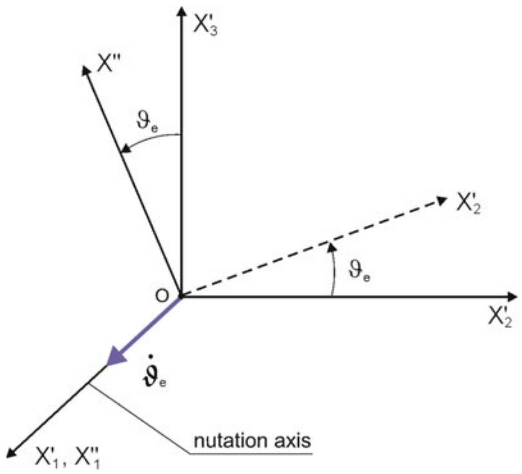

Fig. 2.4 Rotation about nutation angle

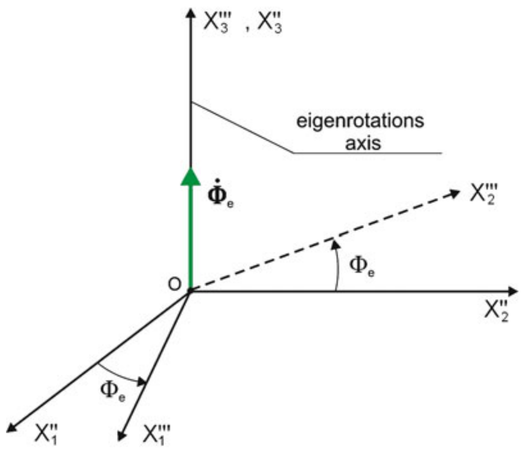

Fig. 2.5 Rotation about the axis of eigenrotations

The corresponding transformation matrix has the following form:

$$m^{\Phi} = \begin{bmatrix} 0 & 0 & 0 \\ \cos \Phi_e & \sin \Phi_e & 0 \\ -\sin \Phi_e & \cos \Phi_e & 1 \end{bmatrix}.$$

Let us determine the cosines of the inclination angles of the axes $OX_1''' OX_2''' OX_3'''$ to $OX_{1O}' OX_{2O}' OX_{3O}'$ (observe that these angles are not equal to $\vartheta_e,\ \psi_e,\ \Phi_e$ except some particular cases). These direction cosines are elements of the matrix of transformation, which can be obtained by successive transformations. Then we have

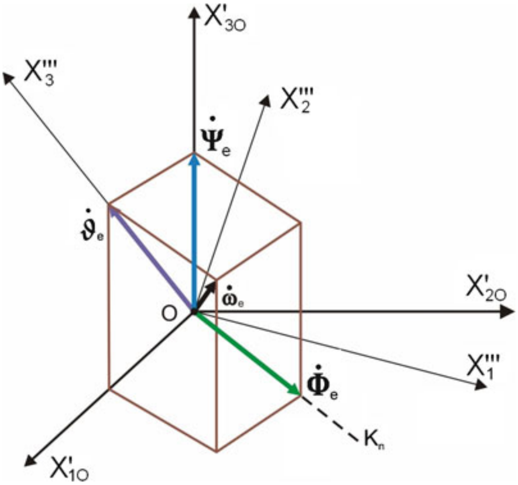

Fig. 2.6 Angular velocity vector of body [1]

$$
\begin{aligned}
m^E &= m^{\Phi}\, m^{\vartheta} m^{\psi} \\
&= \begin{bmatrix} \cos\psi_e & \sin\psi_e & 0 \\ -\sin\psi_e & \cos\psi_e & 0 \\ 0 & 0 & 1 \end{bmatrix} \begin{bmatrix} 1 & 0 & 0 \\ 0 & \cos\vartheta_e & \sin\vartheta_e \\ 0 & -\sin\vartheta_e & \cos\vartheta_e \end{bmatrix} \begin{bmatrix} 0 & 0 & 0 \\ \cos\Phi_e & \sin\Phi_e & 0 \\ -\sin\Phi_e & \cos\Phi_e & 1 \end{bmatrix} \\
&= \begin{bmatrix} \cos\psi_e\cos\Phi_e - \sin\Phi_e\cos\vartheta_e\sin\psi_e & \cos\Phi_e\sin\psi_e + \sin\Phi_e\cos\psi_e\cos\vartheta_e & \sin\Phi_e\sin\vartheta_e \\ -\sin\Phi_e\cos\psi_e - \cos\Phi_e\cos\vartheta_e\sin\psi_e & -\sin\Phi_e\sin\psi_e + \cos\Phi_e\cos\psi_e\cos\vartheta_e & \cos\psi_e\sin\vartheta_e \\ \sin\vartheta_e\sin\psi_e & -\sin\vartheta_e\cos\psi_e & \cos\vartheta_e \end{bmatrix}.
\end{aligned}
\tag{2.1}
$$

The vector $\boldsymbol{\omega}_e$ of the body's angular velocity is a vector sum of the component velocities (Fig. 2.6):

$$
\boldsymbol{\omega}_e = \dot{\boldsymbol{\vartheta}}_e + \boldsymbol{\psi}_e + \dot{\boldsymbol{\Phi}}_e,
\tag{2.2}
$$

where

$$
\dot{\boldsymbol{\vartheta}}_e = \frac{d\boldsymbol{\vartheta}_e}{dt}, \quad \dot{\boldsymbol{\psi}}_e = \frac{\mathrm{d}\boldsymbol{\psi}}{\mathrm{d}t_e}, \quad \dot{\boldsymbol{\Phi}}_e = \frac{\mathrm{d}\boldsymbol{\Phi}}{\mathrm{d}t_e}.
$$

Projections of vector $\boldsymbol{\omega}_e$ onto the OX_1''', OX_2''', and OX_3''' axes are determined in such a way that each of the vectors $\dot{\boldsymbol{\vartheta}}_e$, $\dot{\boldsymbol{\psi}}_e$, and $\dot{\boldsymbol{\Phi}}_e$ is projected onto the aforementioned axes:

$$\boldsymbol{\omega}_e^{OX_1'''X_2'''X_3'''} = m^{\vartheta\Phi}\begin{bmatrix}0\\0\\\dot{\psi}_e\end{bmatrix} + m^{\Phi}\begin{bmatrix}\dot{\vartheta}_e\\0\\0\end{bmatrix} + \begin{bmatrix}0\\0\\\dot{\Phi}_e\end{bmatrix},$$

$$\begin{bmatrix}\omega_{eX_1'''}\\\omega_{eX_2''}\\\omega_{eX_3'''}\end{bmatrix} = \begin{bmatrix}\dot{\Psi}_e\sin\vartheta_e\sin\Phi_e + \dot{\vartheta}_e\cos\Phi_e\\\dot{\psi}_e\sin\vartheta\cos\phi_e - \dot{\vartheta}_e\sin\Phi_e\\\dot{\Phi}_e + \dot{\Phi}_e\cos\vartheta_e\end{bmatrix}. \tag{2.3}$$

The projections of vector $\boldsymbol{\omega}_e$ onto the axes of the fixed frame OX_{1O}', OX_{2O}', OX_{3O}' are as follows:

$$\boldsymbol{\omega}_e^{OX_{1O}'X_{2O}'X_{3O}'} = m^{\psi\vartheta}\begin{bmatrix}0\\0\\\dot{\Phi}_e\end{bmatrix} + m^{\Psi}\begin{bmatrix}\dot{\vartheta}_e\\0\\0\end{bmatrix} + \begin{bmatrix}0\\0\\\dot{\psi}_e\end{bmatrix},$$

$$\begin{bmatrix}\omega_{eX_{1O}'}\\\omega_{eX_{2O}'}\\\omega_{eX_{3O}'}\end{bmatrix} = \begin{bmatrix}\dot{\Phi}_e\sin\vartheta_e\sin\psi_e + \dot{\vartheta}_e\cos\psi_e\\\dot{\Phi}_e\sin\vartheta\cos\psi_e - \dot{\vartheta}_e\sin\psi_e\\\dot{\psi}_e + \dot{\Phi}_e\cos\vartheta_e\end{bmatrix}. \tag{2.4}$$

The preceding formulas (2.3) and (2.4) can be regarded as systems of equations of unknowns $\dot{\vartheta}_e$, $\dot{\psi}_e$, and $\dot{\Phi}_e$. Determining, e.g., on the basis of (2.3), projections of the angular velocities $\dot{\boldsymbol{\vartheta}}_e$, $\dot{\boldsymbol{\psi}}_e$, $\dot{\boldsymbol{\Phi}}_e$ onto the movable axes OX_1''', OX_2''', OX_3''', we have

$$\begin{aligned}\dot{\vartheta}_e &= \omega_{eX_1'''}\cos\Phi_e - \omega_{eX_2'''}\sin\Phi_e,\\ \dot{\psi}_e &= \frac{\omega_{eX_1'''}\sin\Phi_e + \omega_{eX_1'''}\cos\Phi_e}{\sin\vartheta_e},\\ \dot{\Phi}_e &= \omega_{eX_3'''} - \frac{\omega_{eX_1'''}\sin\Phi_e + \omega_{eX_2'''}\cos\Phi_e}{tan\vartheta_e}.\end{aligned} \tag{2.5}$$

Equations (2.5) imply the following conclusions:

(a) For $\vartheta_e = 0$ we have $\dot{\psi}_e$ and $\dot{\Phi}_e$ undetermined.
(b) For $\vartheta_e = \psi_e = \Phi_e = 0$ we have: $\omega_{eX_1'''} = \dot{\vartheta}_e$, $\omega_{eX_2}''' = 0$, $\omega_{eX_3}''' = \dot{\psi}_e + \dot{\Phi}_e$ [(2.3)] regardless of the fact that the values $\dot{\vartheta}_e$, $\dot{\psi}_e$, $\dot{\Phi}_e$ are non-zero, which is not true in a general case.
(c) When $\vartheta_e = 0$, then formulas (2.3) imply that $\omega_{eX_1'''} = -\omega_{eX_2}'''\tan\Phi_e$, which is not valid in a general case either. There are certain paradoxes. Thus, using the Euler angles one should avoid the position of the body at $\vartheta_e = 0$.

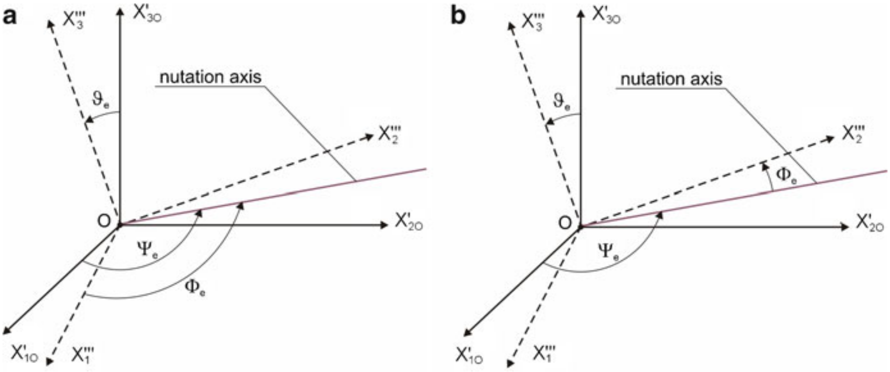

Fig. 2.7 Variants of Euler angles

There exist other variants in specifying angles ψ_e and Φ_e (Fig. 2.7a, b).

Using formulas (2.2), it is possible to determine both the value and direction of the angular velocity $\boldsymbol{\omega}_e$. For the value of the angular velocity ω_e we obtain the expression

$$\omega_e = \sqrt{\omega^2_{eX_1'''} + \omega^2_{eX_2'''} + \omega^2_{eX_3'''}} = \sqrt{\dot{\vartheta}^2_e + \dot{\psi}^2_e + \dot{\Phi}^2_e + 2\dot{\psi}^2_e\dot{\Phi}^2_e \cos\vartheta_e}. \qquad (2.6)$$

The linear velocities of points of a body that rotates about a fixed point O are angular velocities about the instantaneous axis of rotation. This means that the linear velocity $\mathbf{V}_e$ is a cross product of the angular velocity $\boldsymbol{\omega}_e$ of the form [the radius vector $\boldsymbol{\rho}(X_1''', X_2''', X_3''')$ is going to a given point from the fixed point O]

$$\mathbf{V}_e = \boldsymbol{\omega}_e \times \boldsymbol{\rho}_e. \qquad (2.7)$$

Projecting the velocity $\mathbf{V}_e$ onto the OX_1''', OX_2''', OX_3''' axes one obtains

$$\begin{aligned} V_{eX_1'''} &= \omega_{eX_2'''}x_3''' - \omega_{eX_3'''}x_2''', \\ V_{eX_2'''} &= \omega_{eX_3'''}x_1''' - \omega_{eX_1'''}x_3''', \\ V_{eX_3'''} &= \omega_{eX_1'''}x_2''' - \omega_{eX_2'''}x_1'''. \end{aligned} \qquad (2.8)$$

2.1.2 *Cardan Angles*

The appearance of the Cardan angles is connected with the fact of a common spread of the Cardan suspension in gyroscopic devices. The Euler angles ψ_e, ϑ_e, and Φ_e in this kind of device are inconvenient for analysis. This refers to the fact that small movements of the rigid body axis cannot be related to the two small angles from

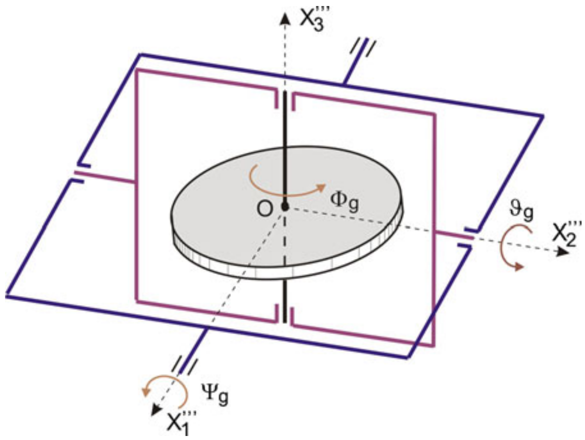

Fig. 2.8 Cardan angles

the following set: ψ_e, ϑ_e, and Φ_e. Moreover, the OX_1''', OX_2''', OX_3''' axes, which are fixed to the body, change their orientation very fast in space at high angular velocities of the body [4,5]. This causes some difficulties in exhibiting various kinds of correcting and control torques, usually about physical axes of the suspension, in the equations of motion of a rigid body. These defects can be eliminated by choosing another set of angles ψ_g, ϑ_g, Φ_g, i.e., the aforementioned Cardan angles compared to ψ_e, ϑ_e, Φ_e.

The Cardan angles can be specified in various ways as angles between particular elements of a suspension. One of the possible forms of a Cardan suspension, along with the assumed angles, is depicted in Fig. 2.8. The Cardan suspension is discussed in more detail subsequently.

Figure 2.8 shows a gyroscope in its initial position, at which the coordinate system $OX_1'''X_2'''X_3'''$, fixed to the rotor, coincides with the fixed system $OX_{1O}'X_{2O}'X_{3O}'$. By mutual rotations of these two bodies, we can specify an arbitrary position of the gyroscope in space, bearing in mind that the origin O remains at rest.

As in the case of the Euler angles, any position of the rotor of the gyroscope can be achieved in the following way (see also [3]):

4. The first rotation is made about the fixed axis (of the external frame) OX_{1O}', by an angle ψ_g (Fig. 2.9). This orthogonal transformation can be expressed by means of a matrix m_g^{ψ} [see (2.9)].
5. The second rotation is made about the internal frame axis OX_1' by an angle ϑ_g (Fig. 2.10). The respective transformation matrix is m_g^{ϑ} [see (2.9)].
6. The final rotation needs to be made about the eigenrotation axis OX_3'' at angle Φ_g (Fig. 2.11). The corresponding transformation matrix is m_g^{Φ} [see (2.9)].

The transformation matrix from the coordinate system OX_{1O}', OX_{2O}', OX_{3O}' to the system OX_1''', OX_2''', OX_3''' has the following form:

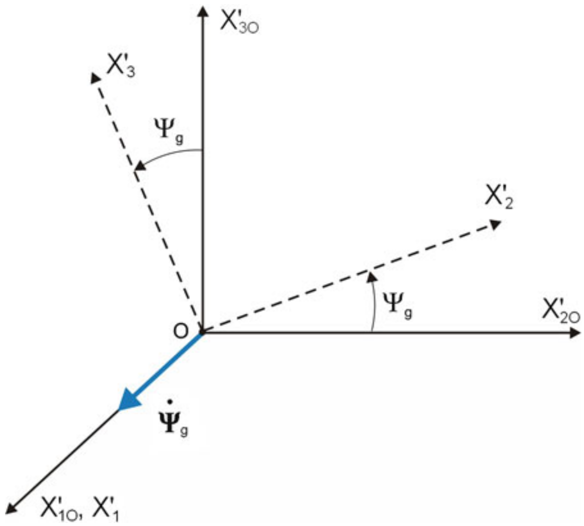

Fig. 2.9 Rotation about external frame axis

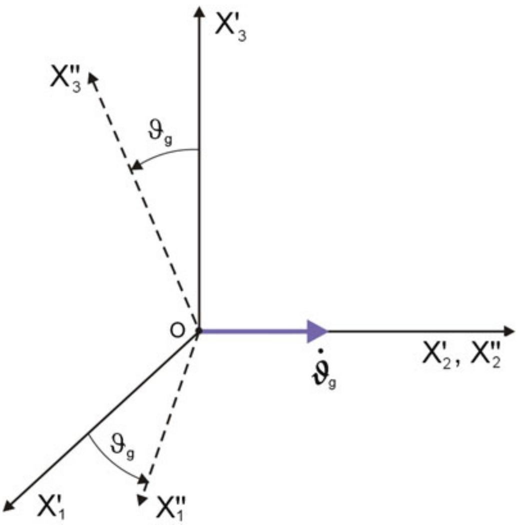

Fig. 2.10 Rotation about internal frame axis

$$
\begin{aligned}
m^K &= m_g^{\psi} m_g^{\vartheta} m_g^{\Phi} \\
&= \begin{bmatrix} 1 & 0 & 0 \\ 0 & \cos\psi_g & \sin\psi_g \\ 0 & -\sin\psi_g & \cos\psi_g \end{bmatrix}
\begin{bmatrix} \cos\vartheta_g & 0 & -\sin\vartheta_g \\ 0 & 1 & 0 \\ \sin\vartheta_g & 0 & \cos\vartheta_g \end{bmatrix}
\begin{bmatrix} \cos\Phi_g & \sin\Phi_g & 0 \\ -\sin\Phi_g & \cos\Phi_g & 0 \\ 0 & 0 & 1 \end{bmatrix}
\end{aligned}
$$

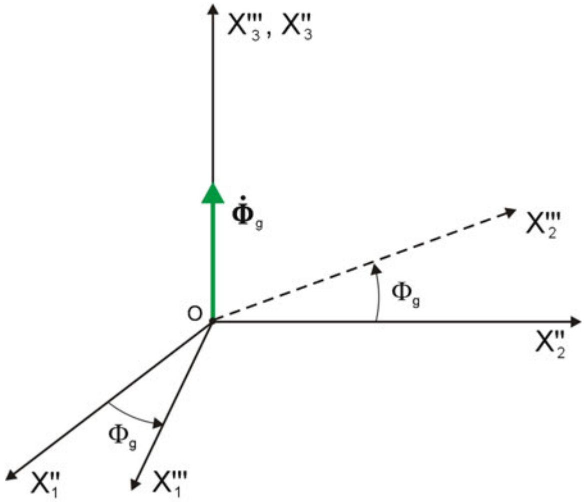

Fig. 2.11 Rotation about eigenrotation axis (fast)

$$= \begin{bmatrix} \cos\psi_g\cos\Phi_g; & \cos\psi_g\sin\Phi_g + \sin\vartheta_g\sin\psi_g\cos\Phi_g; \\ -\sin\psi_g\cos\Phi_g; & \cos\psi_g\cos\Phi_g - \sin\vartheta_g\sin\psi_g\sin\Phi_g; \\ \sin\psi_g; & -\cos\vartheta_g\sin\psi_g; \end{bmatrix}$$

$$\begin{bmatrix} \sin\psi_g\sin\Phi_g - \cos\vartheta_g\sin\psi_g\cos\Phi_g \\ \sin\psi_g\cos\Phi_g + \sin\vartheta_g\cos\psi_g\sin\Phi_g \\ \cos\psi_g\cos\vartheta_g \end{bmatrix}. \tag{2.9}$$

Projections of $\boldsymbol{\omega}_g$ onto the $OX_1''', OX_2''', OX_3'''$ axes are as follows:

$$\boldsymbol{\omega}_g{}^{OX_1'''X_2'''X_3'''} = m_g^{\vartheta\Phi}\begin{bmatrix} \dot\psi_g \\ 0 \\ 0 \end{bmatrix} + m_g^{\Phi}\begin{bmatrix} 0 \\ \dot\vartheta_g \\ 0 \end{bmatrix} + \begin{bmatrix} 0 \\ 0 \\ \dot\Phi_g \end{bmatrix},$$

$$\begin{bmatrix} \omega_{gX_1'''} \\ \omega_{gX_2'''} \\ \omega_{gX_3'''} \end{bmatrix} = \begin{bmatrix} \dot\psi_g\cos\vartheta_g\cos\Phi_g + \dot\vartheta_g\sin\Phi_g \\ -\dot\psi_g\cos\vartheta_g\sin\Phi_g + \dot\vartheta_g\cos\Phi_g \\ \dot\Phi_g + \dot\psi_g\sin\vartheta_g \end{bmatrix}. \tag{2.10}$$

By (2.9) we determine projections of the angular velocities $\dot{\boldsymbol{\vartheta}}_e, \quad \dot{\boldsymbol{\psi}}_e, \quad \dot{\boldsymbol{\Phi}}_e$ onto the movable axes $OX_1''', OX_2''', OX_3'''$, i.e., we obtain

$$\begin{aligned} \dot\vartheta_g &= \omega_{gX_1'''}\sin\Phi_g - \omega_{gX_2'''}\cos\Phi_g, \\ \dot\psi_g &= \frac{\omega_{gX_1'''}\cos\Phi_g - \omega_{gX_2'''}\sin\Phi_g}{\cos\vartheta_g}, \\ \dot\Phi_g &= \omega_{gX_3'''} - \left(\omega_{gX_1'''}\cos\Phi_g - \omega_{gX_2'''}\sin\Phi_g\right)\tan\vartheta_g. \end{aligned} \tag{2.11}$$

Projections of the angular velocity $\boldsymbol{\omega}_g$ described by relations (2.10) [or projections of the angular velocity $\boldsymbol{\omega}_e$ described by relations (2.3)] are not holonomic coordinates in the sense of analytical mechanics. Thus it is not possible to obtain, by means of integration, the angles that could uniquely specify the position of a body in space. That is why one should not measure the components of the angular velocity of a moving object (airplane, missile, bomb, ship) with measurement instruments placed on this object to obtain the rotation angles, by means of direct integration, about the axis of the coordinate system fixed to the object. However, one should integrate a system of non-linear (2.11) [or (2.5)] to determine the aforementioned angles precisely.

In the case of the Cardan angles, we can also observe ambiguities in determining the angular velocities $\dot{\vartheta}_g$, $\dot{\psi}_g$, and $\dot{\Phi}_g$. In a given case it concerns the angle $\vartheta_g = \pi/2$. This corresponds to the case of the so-called frame folding of a Cardan suspension, when the gyroscope fails to operate as a gyroscope.

2.2 Kinetic Energy of a Rigid Body

Considering a body as a set of N material points moving at velocities V_n, we express the kinetic energy of the body as follows [6, 7]:

$$T = \frac{1}{2}\sum_{n=1}^{N} m_n V_n^2. \tag{2.12}$$

Using (2.8), the square of velocity of the nth material point reads

$$\begin{aligned}
V_n^2 &= V_{nX_1'''}^2 + V_{nX_2'''}^2 + V_{nX_3'''}^2 = \left(\omega_{eX_2'''}x_3^n - \omega_{eX_3'''}x_2^n\right)^2 \\
&\quad + \left(\omega_{eX_3'''}x_1^n - \omega_{eX_1'''}x_3^n\right)^2 + \left(\omega_{eX_1'''}x_2^n - \omega_{eX_2'''}x_1^n\right)^2 \\
&= \omega_{eX_1'''}^2\left(\left(x_2^n\right)^2 + \left(x_3^n\right)^2\right) + \omega_{eX_2'''}^2\left(\left(x_3^n\right)^2 + \left(x_1^n\right)^2\right) \\
&\quad + \omega_{eX_3'''}^2\left(\left(x_1^n\right)^2 + \left(x_2^n\right)^2\right) - 2\omega_{eX_2'''}\omega_{eX_3'''}x_2^n x_3^n \\
&\quad - 2\omega_{eX_3'''}\omega_{eX_1'''}x_3^n x_1^n - 2\omega_{eX_1'''}\omega_{eX_2'''}x_1^n x_2^n.
\end{aligned} \tag{2.13}$$

Substituting the preceding expression into (2.12) we obtain

$$\begin{aligned}
T = \frac{1}{2}\Big(& I_{X_1'''}\omega_{eX_1'''}^2 + I_{X_2'''}\omega_{eX_2'''}^2 + I_{X_3'''}\omega_{eX_3'''}^2 - 2I_{yz}\omega_{eX_2'''}\omega_{eX_3'''} \\
& - 2I_{zx}\omega_{eX_3'''}\omega_{eX_1'''} - 2I_{xy}\omega_{eX_1'''}\omega_{eX_2'''}\Big).
\end{aligned} \tag{2.14}$$

As was assumed in our considerations that the axes OX_1''', OX_2''', OX_3''' were fixed to the body and oriented along the main axes of inertia and with the origin at point O, so in this case the moments of inertia $I_{X_1'''}$, $I_{X_2'''}$, $I_{X_3'''}$ are constant and deviation moments equal zero, i.e., $I_{X_2X_3} = I_{X_3X_1} = I_{X_1X_2} = 0$.
Thus, the kinetic energy is expressed in the following form:

$$T = \frac{1}{2}\left(I_{X_1'''}\omega^2_{eX_1'''} + I_{X_2'''}\omega^2_{eX_2'''} + I_{X_3'''}\omega^2_{eX_3'''}\right). \tag{2.15}$$

The kinetic energy of a body—in cases where the body, besides spherical motion, moves in translational motion at the velocity $\mathbf{V}_o$ of its center of mass (by the König theorem)—can be written in the following form:

$$T = \frac{1}{2}m_3 V_o^2 + \frac{1}{2}\left(I_{X_1'''}\omega^2_{eX_1'''} + I_{X_2'''}\omega^2_{eX_2'''} + I_{X_3'''}\omega^2_{eX_3'''}\right). \tag{2.16}$$

2.2.1 Equations of Spherical Motion of a Rigid Body

Let us write a theorem on the variation of the angular momentum in the spherical motion of a body about a fixed point O (center of spherical motion) in the following form (see [1,7] and Chap. 9 of [2]):

$$\frac{\mathrm{d}\mathbf{K}_o}{\mathrm{d}t} = \mathbf{M_o}. \tag{2.17}$$

We find the angular momentum $\mathbf{K}_o$ of the body by the following formula:

$$\begin{aligned}\mathbf{K}_o &= \sum_{n=1}^{N}\boldsymbol{\rho}_n \times m_n\mathbf{V}_n = \sum_{n=1}^{N}\boldsymbol{\rho}_n \times m_n\left(\boldsymbol{\omega}_e \times \boldsymbol{\rho}_n\right)\\ &= \sum_{n=1}^{N} m_n\left[\boldsymbol{\rho}_n \times \left(\boldsymbol{\omega}_e \times \boldsymbol{\rho}_n\right)\right].\end{aligned} \tag{2.18}$$

Using the properties of vector product, (2.18) takes the following form:

$$\begin{aligned}\mathbf{K}_o &= \sum_{n=1}^{N} m_n\left[\boldsymbol{\omega}_e\left(\boldsymbol{\rho}_n \circ \boldsymbol{\rho}_n\right) - \boldsymbol{\rho}_n\left(\boldsymbol{\omega}_e \circ \boldsymbol{\rho}_n\right)\right]\\ &= \sum_{n=1}^{N} m_i\left[\boldsymbol{\omega}_e \circ \rho_n^2 - \rho_n(\boldsymbol{\omega}_e \circ \boldsymbol{\rho}_n)\right]\\ &= \sum_{n=1}^{N} m_n\Big[\boldsymbol{\omega}_e\big((x_1^n)^2 + (x_2^n)^2 + (x_3^n)^2\big) - \boldsymbol{\rho}_n(\omega_{eX_1'''}x_1^n + \omega_{eX_2'''}x_2^n + \omega_{eX_3'''}x_3^n)\Big].\end{aligned} \tag{2.19}$$

In projections onto particular axes of the coordinate system $O_{g3}X_1'''X_2'''X_3'''$, the components of the angular momentum vector read

$$\begin{aligned} K_{X_1'''} &= I_{X_1'''}\omega_{eX_1'''} - I_{X_1X_2}\omega_{eX_2'''} - I_{X_1X_3}\omega_{eX_3'''}, \\ K_{X_2'''} &= I_{X_2'''}\omega_{eX_2'''} - I_{X_2X_3}\omega_{eX_3'''} - I_{yx}\omega_{eX_1'''}, \\ K_{X_3'''} &= I_{X_3'''}\omega_{eX_3'''} - I_{X_3X_1}\omega_{eX_1'''} - I_{X_3X_2}\omega_{eX_2'''}, \end{aligned} \tag{2.20}$$

where

$$\begin{aligned} I_{X_1'''} &= \sum_{n=1}^{N} m_n\left(\left(x_2^n\right)^2 + \left(x_3^n\right)^2\right), \quad & I_{X_2'''} &= \sum_{n=1}^{N} m_n\left(\left(x_3^n\right)^2 + \left(x_2^n\right)^2\right), \\ I_{X_3'''} &= \sum_{n=1}^{N} m_n\left(\left(x_1^n\right)^2 + \left(x_2^n\right)^2\right), \quad & I_{X_1X_2} &= \sum_{n=1}^{N} m_n x_1^n x_2^n, \\ I_{X_2X_3} &= \sum_{n=1}^{N} m_n x_2^n x_3^n, & I_{X_3X_1} &= \sum_{n=1}^{N} m_n x_3^n x_1^n. \end{aligned}$$

In cases where the axes OX_1''', OX_2''', OX_3''' are the main axes intersecting at point O, the moments of deviation of the body relative to these axes read $I_{X_1X_2} = I_{X_2X_3} = I_{X_1X_3} = 0$.

Finally, the components of the angular momentum take the form

$$K_{X_1'''} = I_{X_1'''}\omega_{eX_1'''}, \quad K_{X_2'''} = I_{X_2'''}\omega_{eX_2'''}, \quad K_{X_3'''} = I_{X_3'''}\omega_{eX_3'''}. \tag{2.21}$$

A derivative of the angular momentum $\mathbf{K}_o$ with respect to time has the following form:

$$\begin{aligned} \frac{\mathrm{d}\mathbf{K}_o}{\mathrm{d}t} &= \mathbf{E}_1'''\frac{\mathrm{d}K_{X_1'''}}{\mathrm{d}t} + \mathbf{E}_2'''\frac{\mathrm{d}K_{X_2'''}}{\mathrm{d}t} + \mathbf{E}_3'''\frac{\mathrm{d}K_{X_3'''}}{\mathrm{d}t} + \boldsymbol{\omega}_e \times \mathbf{K}_o \\ &= \mathbf{E}_1'''\frac{\mathrm{d}K_{X_1'''}}{\mathrm{d}t} + \mathbf{E}_2'''\frac{\mathrm{d}K_{X_2'''}}{\mathrm{d}t} + \mathbf{E}_3'''\frac{\mathrm{d}K_{X_3'''}}{\mathrm{d}t} \\ &\quad + \begin{vmatrix} \mathbf{E}_1''' & \mathbf{E}_2''' & \mathbf{E}_3''' \\ \omega_{eX_1'''} & \omega_{eX_2'''} & \omega_{eX_3'''} \\ K_{X_1'''} & K_{X_2'''} & K_{X_3'''} \end{vmatrix}. \end{aligned} \tag{2.22}$$

Equations (2.17), taking into account (2.22) in projections onto the axes of the movable coordinate system $OX_1'''X_2'''X_3'''$, will have the form

$$\begin{aligned}\frac{\mathrm{d}K_{X_1'''}}{\mathrm{d}t} + \omega_{eX_2'''}K_{X_3'''} - \omega_{eX_3'''}K_{X_2'''} &= M_{X_1'''},\\ \frac{\mathrm{d}K_{X_2'''}}{\mathrm{d}t} + \omega_{eX_3'''}K_{X_1'''} - \omega_{eX_1'''}K_{X_3'''} &= M_{X_2'''},\\ \frac{\mathrm{d}K_{X_3'''}}{\mathrm{d}t} + \omega_{eX_1'''}K_{X_2'''} - \omega_{eX_2'''}K_{X_1'''} &= M_{X_3'''}.\end{aligned} \tag{2.23}$$

Assuming that the axes of the movable coordinate system are the main axes of inertia of the body at the point O_{g_3}, we substitute (2.21) into (2.23) and obtain

$$I_{X_1'''}\frac{\mathrm{d}\omega_{eX_1'''}}{\mathrm{d}t} + \left(I_{X_3'''} - I_{X_2'''}\right)\omega_{eX_2'''}\omega_{eX_3'''} = M_{X_1'''}, \tag{2.24a}$$

$$I_{X_2'''}\frac{\mathrm{d}\omega_{eX_2'''}}{\mathrm{d}t} + \left(I_{X_1'''} - I_{X_3'''}\right)\omega_{eX_2'''}\omega_{eX_3'''} = M_{X_2'''}, \tag{2.24b}$$

$$I_{X_3'''}\frac{\mathrm{d}\omega_{eX_3'''}}{\mathrm{d}t} + \left(I_{X_2'''} - I_{X_1'''}\right)\omega_{eX_1'''}\omega_{eX_2'''} = M_{X_3'''}. \tag{2.24c}$$

These are the Euler equations of a rigid body in spherical motion [1, 3, 7, 8]. By adding to the preceding (2.23) the relations among projections of the angular velocities $\omega_{eX_1'''}$, $\omega_{eX_2'''}$, $\omega_{eX_3'''}$, we will obtain six first-order ODEs, which (along with suitable initial conditions) fully govern the rotation of a rigid body about a fixed point. The solution of the non-linear differential (2.24) involves elliptic integrals.

Suppose that the torque $\mathbf{M_o}$ acting on a rigid body is caused by a single gravity force $\mathbf{G} = m\mathbf{g}$. It can thus be presented in the form

$$\mathbf{M_o} = \mathbf{r}_c \times m\mathbf{g} = \begin{vmatrix} \mathbf{E}_1''' & \mathbf{E}_2''' & \mathbf{E}_3''' \\ x_{1C}''' & x_{2C}''' & x_{3C}''' \\ G_{X_1'''} & G_{X_2'''} & G_{X_3'''} \end{vmatrix}, \tag{2.25}$$

where X_{1C}''', X_{2C}'''', X_{3C}''' are coordinates of the center of mass in the coordinate system $OX_1'''X_2'''X_3'''$. Observe that $[G_{X_1'''},\quad G_{X_2'''},\quad G_{X_3'''}]^{\mathrm{T}} = m^E[0,\quad 0,\quad -G]^{\mathrm{T}} = -G[\sin\Phi_e\sin\vartheta_e,\quad \cos\Phi_e\sin\vartheta_e,\quad \cos\vartheta_e]^{\mathrm{T}}$, where m^E is matrix of transformation described by relation (2.1); $\gamma_1,\ \gamma_2,\ \gamma_3$ are direction cosines of the angles between the axis OX_3''' and the axes $OX_1,\ OX_2,\ OX_3$, where

$$\gamma_1 = \sin\Phi_e\sin\vartheta_e, \quad \gamma_2 = \cos\Phi_e\sin\vartheta_e, \quad \gamma_3 = \cos\vartheta_e. \tag{2.26}$$

Taking into account (2.25), the dynamical Euler equations can be cast in the following form:

$$I_{X_1'''}\frac{\mathrm{d}\omega_{eX_1'''}}{\mathrm{d}t}+\left(I_{X_3'''}-I_{X_2'''}\right)\omega_{eX_2'''}\omega_{eX_3'''}=G\left(\gamma_2 x_{3C}'''-\gamma_3 x_{2C}'''\right), \tag{2.27a}$$

$$I_{X_2'''}\frac{\mathrm{d}\omega_{eX_3'''}}{\mathrm{d}t}+\left(I_{X_1'''}-I_{X_3'''}\right)\omega_{eX_1'''}\omega_{eX_3'''}=G\left(\gamma_3 x_{1C}'''-\gamma_1 x_{3C}'''\right), \tag{2.27b}$$

$$I_{X_3'''}\frac{\mathrm{d}\omega_{eX_3'''}}{\mathrm{d}t}+\left(I_{X_2'''}-I_{X_1'''}\right)\omega_{eX_1'''}\omega_{eX_2'''}=G\left(\gamma_1 x_{2C}'''-\gamma_2 x_{1C}'''\right). \tag{2.27c}$$

The derivative of versor $\mathbf{k}$ of OX_3 with respect to time is as follows:

$$\begin{aligned}\frac{\mathrm{d}\mathbf{k}}{\mathrm{d}t}&=\left.\frac{\mathrm{d}\mathbf{k}}{\mathrm{d}t}\right|_{OX_1'''X_2'''X_3'''}+\boldsymbol{\omega}_e\times\mathbf{k}=\frac{\mathrm{d}k_{X_1'''}}{\mathrm{d}t}\mathbf{E}_1'''+\frac{\mathrm{d}k_{X_2'''}}{\mathrm{d}t}\mathbf{E}_2'''+\frac{\mathrm{d}k_{X_3'''}}{\mathrm{d}t}\mathbf{E}_3'''\\
&+\begin{vmatrix}\mathbf{E}_1''' & \mathbf{E}_2''' & \mathbf{E}_3'''\\ \omega_{eX_1'''} & \omega_{eX_2'''} & \omega_{eX_3'''}\\ k_{X_1'''} & k_{X_2'''} & k_{X_3'''}\end{vmatrix}=\left(\frac{\mathrm{d}\gamma_1}{\mathrm{d}t}+\omega_{eX_2'''}\gamma_3-\omega_{eX_3'''}\gamma_2\right)\mathbf{E}_1'''\\
&+\left(\frac{\mathrm{d}\gamma_2}{\mathrm{d}t}+\omega_{eX_3'''}\gamma_1-\omega_{eX_1'''}\gamma_3\right)\mathbf{E}_2'''+\left(\frac{\mathrm{d}\gamma_3}{\mathrm{d}t}+\omega_{eX_1'''}\gamma_3-\omega_{eX_2'''}\gamma_1\right)\mathbf{E}_3''',\end{aligned}$$

and hence

$$\frac{\mathrm{d}\gamma_1}{\mathrm{d}t}=\omega_{eX_3'''}\gamma_2-\omega_{eX_2'''}\gamma_3, \tag{2.28a}$$

$$\frac{\mathrm{d}\gamma_2}{\mathrm{d}t}=\omega_{eX_1'''}\gamma_3-\omega_{eX_3'''}\gamma_1, \tag{2.28b}$$

$$\frac{\mathrm{d}\gamma_3}{\mathrm{d}t}=\omega_{eX_2'''}\gamma_1-\omega_{eX_1'''}\gamma_2. \tag{2.28c}$$

The obtained relations are called the *Poisson equations*. These equations, together with (2.27), form a basic mathematical model of motion of a heavy rigid body about a fixed point; they are called the *Euler–Poisson equations*. The angle ψ_e, which does not occur in (2.28), can be determined by means of quadratures of the *Euler kinematic equations* (2.3). Although one can determine as well the remaining angles Φ_e and ϑ_e from (2.3) knowing the angular velocities $\omega_{eX_1'''}$, $\omega_{eX_2'''}$, and $\omega_{eX_3'''}$, the relationships (2.28) are more advantageous since they require no redundant integrations.

One can show that [1, 3] when four first integrals are found, the problem of solving the system of (2.27) and (2.28) reduces to the quadratures. Three integrals can be determined directly.

Multiplying each equation of system (2.28) by $\gamma_1,\ \gamma_2,\ \gamma_3$, respectively, and adding the equations we obtain a trivial integral

$$\gamma_1^2 + \gamma_2^2 + \gamma_3^2 = 1. \tag{2.29}$$

We obtain the second integral from the obvious relation

$$\frac{\mathrm{d}K_{X_{3O}}}{\mathrm{d}t} = M_{X_{3O}} = 0, \tag{2.30}$$

where $K_{X_{3O}}$ is a projection of the angular momentum of a rigid body onto the OX_{3O} axis in a fixed frame and reads

$$K_{X_{3O}} = K_{X_1'''} \sin\Phi_e \sin\vartheta_e + K_{X_2'''} \cos\Phi_e \sin\vartheta_e + K_{X_3'''} \cos\vartheta_e. \tag{2.31}$$

Taking into account (2.26) and (2.21), we obtain the first integral of the form

$$I_{X_1'''}\omega_{X_1'''}\gamma_1 + I_{X_1'''}\omega_{X_2'''}\gamma_2 + I_{X_3'''}\omega_{X_3'''}\gamma_3 = \text{const.} \tag{2.32}$$

If each equation of system (2.27) is multiplied by $\omega_{eX_1'''}$, $\omega_{eX_2'''}$, and $\omega_{eX_3'''}$, respectively, and the equations are added to one another, then we will obtain the first integral of the kinetic energy:

$$T = \frac{1}{2}\left(I_{X_1'''}\omega^2_{X_1'''} + I_{X_2'''}\omega^2_{X_2'''} + I_{X_3'''}\omega^2_{X_3'''}\right). \tag{2.33}$$

It is easy to see that the potential energy of a rigid body in the considered case reads

$$V = Gx_{3O} = G\left(x_{1C}'''\gamma_1 + x_{2C}'''\gamma_1 + x_{3C}'''\gamma_1\right). \tag{2.34}$$

Thus, by the principle of conservation of energy for a heavy rigid body in spherical motion

$$T + V = \text{const}, \tag{2.35}$$

we obtain the third integral in the form

$$\frac{1}{2}\left(I_{X_1'''}\omega^2_{X_1'''} + I_{X_2'''}\omega^2_{X_2'''} + I_{X_3'''}\omega^2_{X_2'''}\right) + G\left(x_{1C}'''\gamma_1 + x_{2C}'''\gamma_1 + x_{3C}'''\gamma_1\right) = \text{const.} \tag{2.36}$$

A problem related to finding the fourth integral is the essence of solving the Euler–Poisson system of equations. It was precisely this problem that was investigated by Euler, Lagrange, Poinsot, Kovalevskaya, Poincaré, Lyapunov, and many other renowned scientists. Unfortunately, the problem remains unsolved. However, a general solution of these equations has been found only in three cases: Euler ($x_{1C}''' = 0,\ x_{2C}''' = 0,\ x_{3C}''' = 0$); Lagrange ($I_{X_1'''} = I_{X_2'''},\ x_{1C}''' = 0,\ x_{2C}''' = 0$); Kovalevskaya ($I_{X_1'''} = I_{X_2'''} = 2I_{X_3'''},\ x_{3C}''' = 0$); see also the related discussion in [3].

In subsequent subsections, we will consider the aforementioned cases of spherical motion of a rigid body in more detail from the point of view of applications.

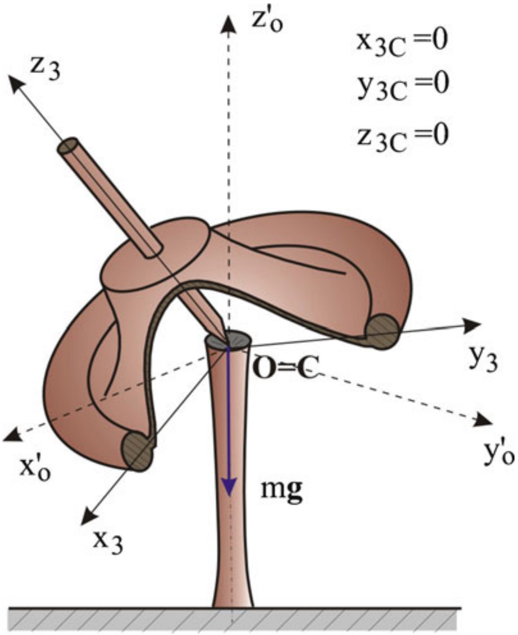

Fig. 2.12 The Euler case

2.2.2 The Euler Case and Geometric Interpretation of Motion of a Body by Poinsot

Consider the motion of a rigid body about a fixed supporting point O. Suppose that the center of mass of this body coincides with the center of rotation at the point O (Fig. 2.12).

If we ignore friction in the bearing, which supports the body and air resistance, then the moments of all external forces about the fixed center of mass O will equal zero. The system of the Euler dynamical equations (2.22) will take the form

$$I_{X_1'''}\frac{\mathrm{d}\omega_{eX_1'''}}{\mathrm{d}t} + \left(I_{X_3'''} - I_{X_2'''}\right)\omega_{eX_2'''}\omega_{eX_3'''} = 0, \tag{2.37a}$$

$$I_{X_2'''}\frac{\mathrm{d}\omega_{eX_2'''}}{\mathrm{d}t} + \left(I_{X_1'''} - I_{X_3'''}\right)\omega_{eX_1'''}\omega_{eX_3'''} = 0, \tag{2.37b}$$

$$I_{X_3'''}\frac{\mathrm{d}\omega_{eX_3'''}}{\mathrm{d}t} + \left(I_{X_2'''} - I_{X_1'''}\right)\omega_{eX_1'''}\omega_{eX_2'''} = 0. \tag{2.37c}$$

Note that it is not difficult to find two integrals of (2.37). To find the first integral, let us multiply the first of these equations by $\omega_{eX_1'''}$, the second one by $\omega_{eX_2'''}$, and the third one by $\omega_{eX_3'''}$ and then add them all up. Then we obtain

$$I_{X_1'''}\omega_{eX_1'''}\dot{\omega}_{eX_1'''} + I_{X_2'''}\omega_{eX_2'''}\dot{\omega}_{eX_2'''} + I_{X_3'''}\omega_{eX_3'''}\dot{\omega}_{eX_3'''} = 0. \tag{2.38}$$

The preceding equation is transformed into the form

$$\frac{1}{2}\frac{\mathrm{d}}{\mathrm{d}t}\left(I_{X_1'''}\omega^2_{eX_1'''} + I_{X_2'''}\omega^2_{eX_2'''} + I_{X_3'''}\omega^2_{eX_3'''}\right) = 0. \tag{2.39}$$

Hence we have

$$I_{X_1'''}\omega^2_{eX_1'''} + I_{X_2'''}\omega^2_{eX_2'''} + I_{X_3'''}\omega^2_{eX_3'''} = \text{const.} \tag{2.40}$$

The expression on the left-hand side of (2.40) is equal to a doubled kinetic energy of the considered body, governed by formula (2.35). Thus we have shown that in the given case, the kinetic energy is constant $T = T^o = \text{const}$. The latter observation is obviously consistent with the theorem on kinetic energy when external forces acting on the body do not undertake any work. Let us write (2.40) in the form

$$\begin{aligned} &I_{X_1'''}\omega^2_{eX_1'''} + I_{X_2'''}\omega^2_{eX_2'''} + I_{X_3'''}\omega^2_{eX_3'''} \\ &\quad = K_{X_1'''}\omega_{eX_1'''} + K_{X_2'''}\omega_{eX_2'''} + K_{X_3'''}\omega_{eX_3'''} = 2T^o. \end{aligned} \tag{2.41}$$

It follows from (2.41) that the end of vector $\boldsymbol{\omega}_e$ can move only in the plane perpendicular to $\mathbf{K}_o$.

We are left to find the second integral. This time, let us multiply (2.37a) by $K_{X_1'''} = I_{X_1'''}\omega_{eX_1'''}$, (2.37b) by $K_{X_2'''} = I_{X_2'''}\omega_{eX_2'''}$, and (2.37c) by $K_{X_3'''} = I_{X_3'''}\omega_{eX_3'''}$ and add them up. Then we obtain

$$I^2_{X_1'''}\omega_{eX_1'''}\frac{\mathrm{d}\omega_{eX_1'''}}{\mathrm{d}t} + I^2_{X_2'''}\omega_{eX_2'''}\frac{\mathrm{d}\omega_{eX_2'''}}{\mathrm{d}t} + I^2_{X_3'''}\omega_{eX_3'''}\frac{\mathrm{d}\omega_{eX_3'''}}{\mathrm{d}t} = 0. \tag{2.42}$$

Equation (2.42) is equivalent to

$$\frac{\mathrm{d}}{\mathrm{d}t}\left(I^2_{X_1'''}\omega^2_{eX_1'''} + I^2_{X_2'''}\omega^2_{eX_2'''} + I^2_{X_3'''}\omega^2_{eX_3'''}\right) = 0. \tag{2.43}$$

Note that the expression in parentheses in (2.43) is equal to the square of the absolute value of the angular momentum $\mathbf{K}_o$ relative to point O. Thus, we obtain the following integral of (2.43):

$$I^2_{X_1'''}\omega^2_{eX_1'''} + I^2_{X_2'''}\omega^2_{eX_2'''} + I^2_{X_3'''}\omega^2_{eX_3'''} = K_o^2 = \text{const.} \tag{2.44}$$

This time it was shown that the magnitude of the angular momentum relative to point O is constant.

Although the first two integrals (2.42) and (2.44) do not allow one to obtain the components of the angular velocity $\boldsymbol{\omega}_e$ as a function of time t, they provide a simple geometric interpretation that was first studied by Poinsot. Note that (2.41) describes the energy ellipsoid, which can be written in the form

$$\left(\frac{\omega_{eX_1'''}}{a_e}\right)^2 + \left(\frac{\omega_{eX_2'''}}{b_e}\right)^2 + \left(\frac{\omega_{eX_3'''}}{c_e}\right)^2 = 1, \tag{2.45}$$

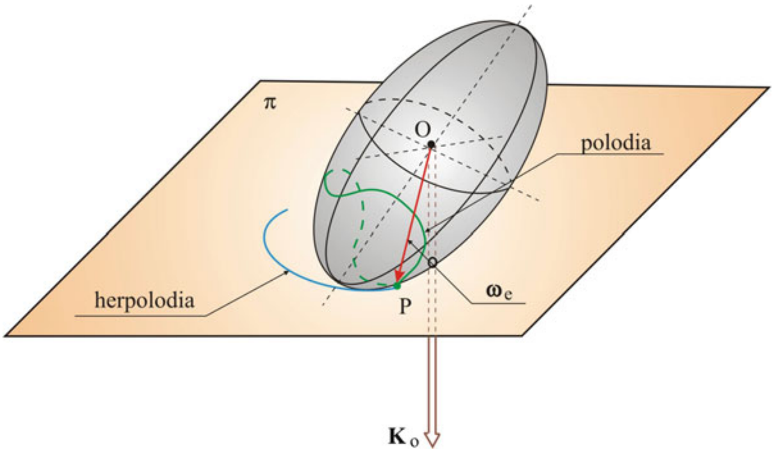

Fig. 2.13 Rolling of energy ellipsoid on a fixed plane

where the semiaxes are as follows:

$$a_e = \sqrt{\frac{2T^o}{I_{X_1'''}}}, \quad b_e = \sqrt{\frac{2T^o}{I_{X_2'''}}}, \quad c_e = \sqrt{\frac{2T^o}{I_{X_3'''}}}.$$

Ellipsoid (2.45) is a locus of ends of the vector $\boldsymbol{\omega}_e$ (it corresponds to the constant kinetic energy T^o). The main axes of the energy ellipsoid are simultaneously main axes of the body, whose center coincides with the supporting point O (Fig. 2.13). Equation (2.44) describes the kinetic ellipsoid, which is a locus of ends of vector $\boldsymbol{\omega}_e$ (it corresponds to the constant angular momentum).

The invariant plane π and ellipsoid (2.45) touch each other at point P, which is an end of vector $\boldsymbol{\omega}_e$. Since the angular momentum $\mathbf{K}_o$ is permanently perpendicular to the plane π, this plane is tangent to the energy ellipsoid at point P. The ellipsoid rolls without slip on the plane because point P lies on the instantaneous axis, which is why its velocity equals zero. During this rolling, pole P draws on the plane $\boldsymbol{\pi}$, a curve called a *herpolodia*, while on an energy ellipsoid a curve, it is known as a *polodia* (Fig. 2.13).

Polodias are closed curves on the surface of an energy ellipsoid. We can determine them as curves of intersection between the ellipsoid described by (2.41) and the kinetic ellipsoid described by (2.44). Shapes of polodias can be viewed by means of their projections onto the main planes $OX_1'''X_2'''$, $OX_1'''X_3'''$, and $OX_2'''X_3'''$. Making appropriate transformations of (2.41) and (2.44) we obtain

$$I_{X_2'''}\left(I_{X_1'''} - I_{X_2'''}\right)\omega_{eX_2'''}^2 + I_{X_3'''}\left(I_{X_1'''} - I_{X_3'''}\right)\omega_{eX_3'''}^2 = 2T^o I_{X_1'''} - K_o^2, \tag{2.46a}$$

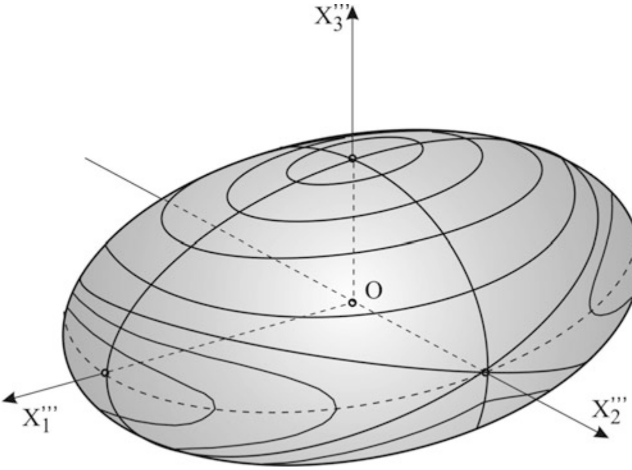

Fig. 2.14 Rolling of energy ellipsoid on invariant plane

$$-I_{X_1'''}\left(I_{X_1'''}-I_{X_2'''}\right)\omega_{eX_1'''}^2+I_{X_3'''}\left(I_{X_2'''}-I_{X_3'''}\right)\omega_{eX_3'''}^2=2T^oI_{X_2'''}-K_o^2, \tag{2.46b}$$

$$-I_{X_1'''}\left(I_{X_1'''}-I_{X_3'''}\right)\omega_{eX_1'''}^2-I_{X_3'''}\left(I_{X_2'''}-I_{X_3'''}\right)\omega_{eX_2'''}^2=2T^oI_{X_3'''}-K_o^2. \tag{2.46c}$$

If we choose the main axes so that $I_{X_1'''} > I_{X_2'''} > I_{X_3'''}$, then (2.46) imply that in the planes $OX_2'''X_3'''$ and $OX_1'''X_2'''$, projections of polodia are ellipses, whereas in the plane $OX_1'''X_3'''$ they are hiperbolas (Fig. 2.14). In a projection onto the plane $OX_1'''X_3'''$ the boundary curves reduce to straight lines, which are asymptotes of hyperbola families. From (2.46b) we easily determine equations of these asymptotes:

$$\omega_{eX_1'''}=\pm\sqrt{\frac{I_{X_3'''}\left(I_{X_2'''}-I_{X_3'''}\right)}{I_{X_1'''}\left(I_{X_1'''}-I_{X_2'''}\right)}}\omega_{eX_3'''}. \tag{2.47}$$

When $I_{X_2'''} = I_{X_3'''}$, then a direction coefficient of a straight line equals zero, and if $I_{X_1'''} = I_{X_2'''}$, then the coefficient tends to infinity, which corresponds to the inclination angle of the line, namely, $\pi/2$. In the former case we are dealing with a flatten rotational ellipsoid, whereas in the second case we are dealing with a lengthened rotational ellipsoid with respect to its symmetry axis.

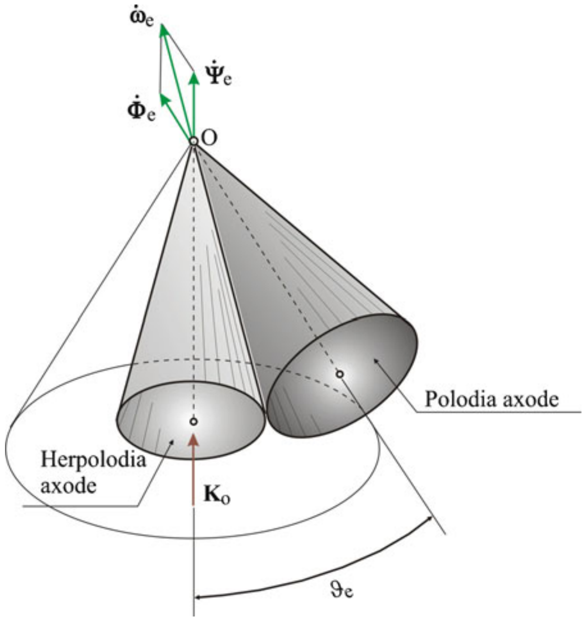

Fig. 2.15 Rolling of energy ellipsoid on invariant plane

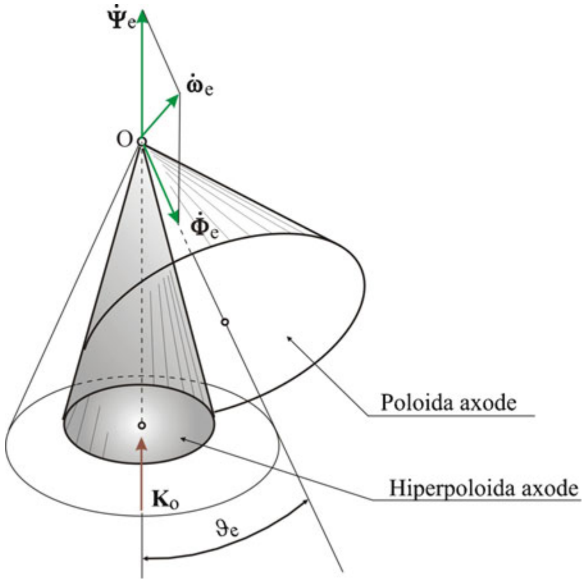

Fig. 2.16 Rolling of energy ellipsoid on invariant plane

Polodias and herpolodias are directrices of two cones of a common vertex at point O. During the motion of the analyzed body the polodia cone becomes a movable axode, which rolls without sliding on a herpolodia cone, which is a fixed axode (Figs. 2.15 and 2.16).

Suppose that a rigid body with a fixed center of mass is axially symmetric $I_{X_2'''} = I_{X_3'''} = I_b$ (its central inertial ellipsoid is a rotational ellipsoid) and rotates about both a movable axis OX_1''' at angular velocity $\dot{\Phi}_e$ and a fixed axis OX_{3O} at angular velocity $\dot{\psi}_e$. Then, the ellipsoid rolls on the invariant plane $\boldsymbol{\pi}$ perpendicular to the constant angular momentum $\mathbf{K}_o$. In this case, all possible polodias are circles lying in planes perpendicular to the axis OX_1''', and herpolodias, which are also circles, are perpendicular to the axis OX_{3O}. Moreover, both movable and immovable axodes are cones simple circular with common vertex O (center of mass of the rigid body).

Figure 2.15 presents a case of motion of an oblate ellipsoid, i.e., when $I_{X_1'''} > I_b$. Then the movable axode moves outside on the surface of the immovable axode. In Fig. 2.16, the case of the lengthened ellipsoid is depicted ($I_{X_1'''} > I_b$), for which the fixed axode is located inside the movable axode rolling on the external surface.

As was already mentioned, Euler considered inertial motion of a body, i.e. the one, in which the sole force acting on the body is gravity at the fixed center of mass. In this case

$$M_{X_1'''} = M_{X_2'''} = M_{X_3'''} = 0. \tag{2.48}$$

Moreover, he assumed that a body was symmetric relative to the axis OX_3''', i.e., $I_{X_1'''} = I_{X_2'''}$. In this case we have

$$\tfrac{1}{2}\left[I_{X_1'''}\left(\omega^2_{X_1'''} + \omega^2_{X_2'''}\right) + I_{X_3'''}\omega^2_{X_3'''}\right] = T^o = \text{const}, \tag{2.49a}$$

$$I_{X_1'''}\left(\omega^2_{X_1'''} + \omega^2_{X_2'''}\right) + I_{X_3'''}\omega^2_{X_3'''} = K_o^2 = \text{const}, \tag{2.49b}$$

$$\omega_{X_3'''} = \omega^o_{X_3'''} = \text{const}. \tag{2.49c}$$

For this particular case the angular momentum $\mathbf{K}_o$ is constant, both the norm and the direction relative to the fixed coordinate system. In projections onto the fixed axes of the coordinate system vector $\mathbf{K}_o$ is as follows:

$$K_{X_1} = K_o \sin\vartheta_e \sin\Phi_e = I_{X_1'''}\omega_{X_1'''}, \tag{2.50a}$$

$$K_{X_2} = K_o \sin\vartheta_e \cos\Phi_e = I_{X_2'''}\omega_{X_2'''}, \tag{2.50b}$$

$$K_{X_3} = K_o \cos\vartheta_e = I_{X_3'''}\omega^o_{X_3'''}. \tag{2.50c}$$

By (2.50c) we have

$$\cos\vartheta_e = \frac{I_{X_3'''}\omega^o_{X_3'''}}{K_o} = \text{const}; \quad \vartheta_e = \vartheta_e^o = \text{const}; \quad \frac{\mathrm{d}\vartheta_e}{\mathrm{d}t} = 0. \tag{2.51}$$

Taking into account (2.51), formulas (2.49) and (2.50) can be expressed in the following form:

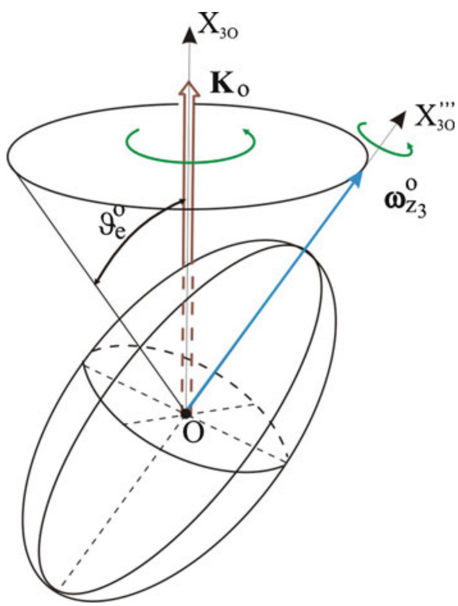

Fig. 2.17 Regular precession for the Euler case

$$\omega_{X_1'''} = \dot{\psi}_e \sin\vartheta_e \sin\Phi_e, \tag{2.52a}$$

$$\omega_{X_2'''} = \dot{\psi}_e \sin\vartheta_e \cos\Phi_e, \tag{2.52b}$$

$$\omega_{X_3'''} = \dot{\psi}_e \cos\vartheta_e + \dot{\Phi}_e, \tag{2.52c}$$

$$K_{X_1} = I_{X_1'''}\dot{\psi}_e \sin\vartheta_e^o \sin\Phi_e = K_o \sin\vartheta_e^o \sin\Phi_e; \quad I_{X_1'''}\dot{\psi}_e = K_o, \tag{2.53a}$$

$$K_{X_1} = I_{X_1'''}\dot{\psi}_e \sin\vartheta_e^o \cos\Phi_e = K_o \sin\vartheta_e^o \cos\Phi_e; \quad I_{X_1'''}\dot{\psi}_e = K_o. \tag{2.53b}$$

Equations (2.53a) and (2.53b) became identical, hence

$$\dot{\psi}_e = \frac{K_o}{I_{X_1'''}} = \text{const} = n_1; \quad \psi_e = n_1 t + \psi_e^o, \tag{2.54}$$

while from (2.52c) we have

$$\dot{\Phi}_e = \omega_{X_3'''}^o - n_1 \cos\vartheta_e^o = \text{const} = n_2; \quad \Phi_e = n_2 t + \Phi_e^o. \tag{2.55}$$

Thus, the Euler case presents the regular precession (Fig. 2.17).

Fig. 2.18 Lagrange case

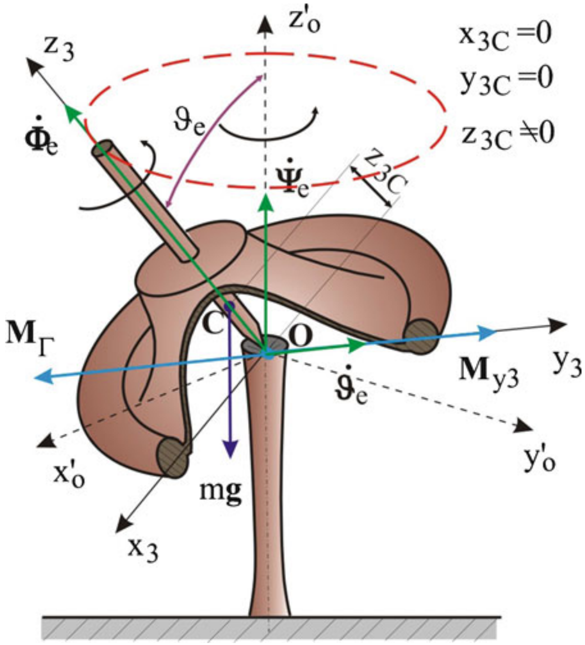

2.2.3 Lagrange Case (Pseudoregular Precession)

Consider the motion of a rigid body about a fixed pivot point for a case investigated by Lagrange. The case relies on the fact that the analyzed body is axially symmetric (the respective inertial ellipsoid is a prolate spheroid) $I_{X_1'''} = I_{X_2'''}$. The supporting point (rotation) O and center of mass C lie on the body's axis of symmetry, where $OC = X_{3C}'''$, and the body is under the influence only of gravitational forces. The body rotates at high angular velocity $\dot{\Phi}_e$ about the symmetry axis OX_3''' (Fig. 2.18). This kind of body is called a gyroscope, and in the given case we can call it the Lagrange gyroscope (a more detailed definition of a gyroscope will be given subsequently). Besides rotating about its own axis of symmetry, the body can rotate about the fixed axis OX_{3O} at angular velocity $\dot{\psi}_e$.

To analyze motion of the Lagrange gyroscope, we introduce two movable coordinate systems $OX_1''X_2''X_3''$ and $OX_1'''X_2'''X_3'''$, which slightly differ from the Euler case considered earlier. Similarly, we will select the axis OX_3'' as a symmetry axis of the body (Fig. 2.18). The axis OX_2'' lies on the line of nodes and the axis OX_1'' is selected in such a way that we obtain a rectangular coordinate system. The frame $OX_1'''X_2'''X_3'''$ is obtained by rotating the frame $OX_1''X_2''X_3''$ by an angle Φ_e about the axis OX_3''.

The matrices of transformation m_2^L and m_3^L from the fixed frame $OX_{1O}X_{2O}\ X_{3O}$ to movable ones $OX_1'''X_2'''X_3'''$ and $OX_1'''X_2'''X_3'''$ will take the forms

$$m_2^L = m^\vartheta m^\psi = \begin{bmatrix} \cos\vartheta_e \cos\psi_e & \cos\vartheta_e \sin\psi_e & -\sin\vartheta_e \\ -\sin\vartheta_e & \cos\psi_e & 0 \\ \sin\vartheta_e \cos\psi_e & \sin\vartheta_e \sin\psi_e & \cos\vartheta_e \end{bmatrix}, \tag{2.56a}$$

$$m_3^L = m^\Phi m^\vartheta m^\psi$$
$$= \begin{bmatrix} \begin{array}{l}\cos\vartheta_e \cos\psi_e \cos\Phi_e + \\ -\cos\vartheta_e \sin\psi_e \sin\Phi_e;\end{array} & \begin{array}{l}\cos\vartheta_e \cos\psi_e \sin\Phi_e + \\ +\cos\vartheta_e \sin\psi_e \cos\Phi_e;\end{array} & -\sin\vartheta_e \\ \\ \begin{array}{l}-\sin\vartheta_e \cos\Phi_e + \\ -\cos\psi_e \sin\Phi_e;\end{array} & \begin{array}{l}-\sin\vartheta_e \sin\Phi_e + \\ +\cos\psi_e \cos\Phi_e;\end{array} & 0 \\ \\ \begin{array}{l}\sin\vartheta_e \cos\psi_e \cos\Phi_e + \\ -\sin\vartheta_e \sin\psi_e \sin\Phi_e;\end{array} & \begin{array}{l}\sin\vartheta_e \cos\psi_e \sin\Phi_e + \\ +\sin\vartheta_e \sin\psi_e \cos\Phi_e;\end{array} & \cos\vartheta_e \end{bmatrix}. \tag{2.56b}$$

We determine projections of the instantaneous angular velocity $\boldsymbol{\omega}_e$ as a result of composing three rotations about the particular axes of both assumed frames.

$$\boldsymbol{\omega}_e = \dot{\boldsymbol{\psi}}_e + \dot{\boldsymbol{\vartheta}}_e + \dot{\boldsymbol{\Phi}}_e. \tag{2.57}$$

Thus, projections onto the axes $OX_1'''X_2'''X_3'''$ of the components of the vector $\boldsymbol{\omega}_e$ are as follows:

$$\boldsymbol{\omega}_e^{OX_1'''X_2'''X_3'''} = m_3^L \begin{bmatrix} 0 \\ 0 \\ \dot{\psi}_e \end{bmatrix} + m_2^L \begin{bmatrix} 0 \\ \dot{\vartheta}_e \\ 0 \end{bmatrix} + \begin{bmatrix} 0 \\ 0 \\ \dot{\Phi}_e \end{bmatrix}, \tag{2.58}$$

$$\omega_{eX_1'''} = -\dot{\psi}_e \sin\vartheta_e, \tag{2.59a}$$

$$\omega_{eX_2'''} = \dot{\vartheta}_e, \tag{2.59b}$$

$$\omega_{eX_3'''} = \dot{\psi}_e \cos\vartheta_e + \dot{\Phi}_e. \tag{2.59c}$$

On the other hand, projections onto the axes $OX_1''X_2''X_3''$ yield

$$\boldsymbol{\omega}_e^{OX_1''X_2''X_3''} = m_2^L \begin{bmatrix} 0 \\ 0 \\ \dot{\psi}_e \end{bmatrix} + \begin{bmatrix} 0 \\ \dot{\vartheta}_e \\ 0 \end{bmatrix} + \begin{bmatrix} 0 \\ 0 \\ 0 \end{bmatrix},$$

$$\omega_{eX_1''} = -\dot{\psi}_e \sin\vartheta_e, \tag{2.60a}$$

$$\omega_{eX_2''} = \dot{\vartheta}_e, \tag{2.60b}$$

$$\omega_{eX_3'''} = \dot{\psi}_e \cos\vartheta_e. \tag{2.60c}$$

At an arbitrary position of the body, the axes $OX_1'''X_2'''X_3'''$ are the main axes of inertia, which is why the angular momentum $\mathbf{K}_o$ components of this body can be cast in the form

$$K_{X_1'''} = I_{X_1'''}\omega_{X_1'''}, \quad K_{X_2'''} = I_{X_2'''}\omega_{X_2'''}, \quad K_{X_3'''} = I_{X_3'''}\omega_{X_3'''}. \tag{2.61}$$

Making use of the theorem on angular momentum change, the equations of motion of Lagrange's gyroscope are written in the form

$$\frac{\mathrm{d}\mathbf{K}_o}{\mathrm{d}t} + \begin{vmatrix} \mathbf{E}_1''' & \mathbf{E}_2''' & \mathbf{E}_3''' \\ \omega_{X_1''} & \omega_{X_2''} & \omega_{X_3''} \\ I_{X_1'''}\omega_{X_1'''} & I_{X_2'''}\omega_{X_2'''} & I_{X_3'''}\omega_{X_3'''} \end{vmatrix} = \mathbf{M_o}.$$

Taking into account the fact that the components of the main moment $\mathbf{M_o}$ of external forces acting on a body have the form

$$\begin{bmatrix} M_{X_1'''} \\ M_{X_2'''} \\ M_{X_3'''} \end{bmatrix} = \begin{vmatrix} \mathbf{E}_1''' & \mathbf{E}_2''' & \mathbf{E}_3''' \\ 0 & 0 & x_{3C}''' \\ G\sin\vartheta_e & 0 & -G\cos\vartheta_e \end{vmatrix} = \begin{bmatrix} 0 \\ Gx_{3C}'''\sin\vartheta_e \\ 0 \end{bmatrix}, \tag{2.62}$$

and taking into account relations (2.49) and (2.50), the equations of motion of the Lagrange gyroscope (2.61),

$$\ddot{\psi}_e\sin\vartheta_e + 2\dot{\psi}_e\dot{\vartheta}_e\cos\vartheta_e - \frac{I_{X_3'''}}{I_{X_1'''}}\left(\dot{\psi}_e\cos\vartheta_e + \dot{\Phi}_e\right)\dot{\vartheta}_e = 0, \tag{2.63a}$$

$$\ddot{\vartheta}_e + \left[\frac{I_{X_3'''}}{I_{X_2'''}}\dot{\Phi}_e + \frac{I_{X_3'''} - I_{X_1'''}}{I_{X_2'''}}\dot{\psi}_e\cos\vartheta_e\right]\dot{\psi}_e\sin\vartheta_e = \frac{Gx_{3C}'''}{I_{X_2'''}}\sin\vartheta_e, \tag{2.63b}$$

$$\frac{\mathrm{d}}{\mathrm{d}t}\left(\dot{\psi}_e\cos\vartheta_e + \dot{\Phi}_e\right) = 0; \quad \dot{\psi}_e\cos\vartheta_e + \dot{\Phi}_e = \omega_o = \mathrm{const}. \tag{2.63c}$$

Let us introduce designation $\dot{\psi} = \omega_1$ and transform (2.53a) into the form of a linear differential equation with respect to angular velocity ω_1:

$$\frac{\mathrm{d}\omega_1}{\mathrm{d}\vartheta_e} + 2\omega_1 ctan\vartheta_e = \frac{I_{X_3'''}\omega_o}{I_{X_1'''}\sin\vartheta_e}. \tag{2.64}$$

It is easy to determine by integration of (2.64)

$$\omega_1 = \frac{C - I_{X_3'''}\omega_o\cos\vartheta_e}{I_{X_1'''}\sin^2\vartheta_e}, \tag{2.65}$$

where C is an integration constant.

In order that a body in the Lagrange case could move in a regular precession (regular precession), the angular velocity ω_1 in this motion should be constant, –$\omega_1 = \text{const} = \dot{\psi}_e^o$. This implies, as shown clearly in (2.65), that angle ϑ_e will also be constant –$\vartheta_e = \text{const} = \vartheta_e^o$. Then, (2.53b) will be simplified to the following form:

$$\left[I_{X_3'''} - \left(I_{X_1'''} - I_{X_3'''} \right) \frac{\omega_1}{\omega_o} \cos \vartheta_e^o \right] \omega_1 \omega_o \sin \vartheta_e^o = G x_{3C}''' \sin \vartheta_e^o. \tag{2.66}$$

Taking into account that the angular velocity of eigenrotations ω_o takes large values, i.e., $\omega_1/\omega_o \ll 1$, (2.66) can be written in a simpler form:

$$G x_{3C}''' \sin \vartheta_e^o - I_{X_3'''} \omega_1 \omega_o \sin \vartheta_e^o = 0, \quad \mathbf{M}_g + I_{X_3'''} \boldsymbol{\omega}_o \times \boldsymbol{\omega}_1 = \mathbf{0},$$
$$\mathbf{M}_g + \mathbf{M}_\Gamma = \mathbf{0}. \tag{2.67}$$

We have obtained the equation of equilibrium of moments of external forces acting on the gyroscope $\mathbf{M}_g$ (in this case the moment of gravitation $M_g = G x_{3C}''' \sin \vartheta_e^o$) and moment of inertial forces $\mathbf{M}_\Gamma$ generated by rotational motion about the symmetry axis $O_{X_3'''}$. The aforementioned torque

$$\mathbf{M}_\Gamma = I_{X_3'''} \boldsymbol{\omega}_o \times \boldsymbol{\omega}_1 \tag{2.68}$$

is called a *gyroscopic moment*.

The formula on the gyroscopic moment can be obtained from (2.66) when the nutation angle equals $\vartheta_e = \pi/2$, i.e., when the angular velocity vector of eigenrotations of the gyroscope is perpendicular to the angular velocity vector of precession $\omega_1 = \dot{\psi}_e$. In this case, exact and approximated formulas are the same. From (2.67) we can determine the precession speed of the Lagrange gyroscope

$$\omega_1 = \dot{\psi}_e = \frac{M_g}{I_{X_3'''} \omega_o} = \frac{G x_{3C}'''}{I_{X_3'''} \dot{\Phi}_e}. \tag{2.69}$$

Let us rewrite (2.66), ignoring $\sin \vartheta_e$, in the following form:

$$\left[I_{X_3'''} \omega_o - \left(I_{X_1'''} - I_{X_3'''} \right) \dot{\psi}_e^o \cos \vartheta_e^o \right] \dot{\psi}_e^o = G x_{3C}'''. \tag{2.70}$$

Solving the preceding equation with respect to $\dot{\psi}_e^o$ we find

$$\dot{\psi}_{ei}^o = \frac{I_{X_3'''} \omega_o \mp \sqrt{I_{X_3'''}^2 \omega_o^2 - 4 \left(I_{X_1'''} - I_{X_3'''} \right) G x_{3C}''' \cos \vartheta_e^o}}{2 \left(I_{X_1'''} - I_{X_3'''} \right) \cos \vartheta_e^o}, \qquad i = 1, 2. \tag{2.71}$$

This implies that solutions exist when

$$I_{X_3'''}^2 \omega_o^2 - 4 \left(I_{X_1'''} - I_{X_3'''} \right) G x_{3C}''' \cos \vartheta_e^o > 0. \tag{2.72}$$

Inequality (2.72) will be preserved if the angular momentum of the Lagrange gyroscope $I^2_{X_3'''}\omega_o^2$ is sufficiently large. This is simultaneously a condition of realization of the regular precession of a gyroscope. Equation (2.71) shows that at a given numerical value of the angular velocity of eigenrotations ω_o, there are three possible types of precession of the examined body. To analyze the obtained result, let us substitute the square root in (2.71) with an approximated expression

$$\sqrt{I^2_{X_3'''}\omega_o^2 - 4\left(I_{X_1'''} - I_{X_3'''}\right) G x_{3C}''' \cos\vartheta_e^o}$$
$$\cong I_{X_3'''}\omega_o - \frac{2\left(I_{X_1'''} - I_{X_3'''}\right) G x_{3C}''' \cos\vartheta_e^o}{I_{X_3'''}\omega_o}. \tag{2.73}$$

Replacing the square root in (2.71) with its approximated value (2.73), we obtain the two following values of the angular velocity of precession:

$$\dot{\psi}_{e1}^o \cong \frac{G x_{3C}'''}{I_{X_1'''}\omega_o}, \qquad \dot{\psi}_{e2}^o \cong \frac{I_{X_1'''}\omega_o}{\left(I_{X_1'''} - I_{X_3'''}\right)\cos\vartheta_e^o}. \tag{2.74}$$

The obtained expressions are two kinds of precession: precession of the first kind (*slow precession*) $\dot{\psi}_{e1}^o$ and precession of the second kind (*fast precession*) $\dot{\psi}_{e2}^o$.

The determined quantities $\dot{\psi}_e^o$, ω_o and ϑ_e^o can be considered initial conditions for equations of motion of the Lagrange gyroscope (2.63). Given these initial conditions and assuming that the motion of the body differs slightly from the regular precession $\left(\vartheta_e = \vartheta_e^o + \Delta\vartheta_e,\right.$ where $\Delta\vartheta_e$ is sufficiently small), (2.63) govern the vibrations of a rigid body about the operation position (stationary), which is the regular precession described previously. The aforementioned vibrations have bounded amplitude and high frequency. The vibrations are called *nutation vibrations*. Thus, we have a superposition of fast vibrations (nutation) and slow vibrations (regular precession). This situation is depicted in Fig. 2.19.

In this figure, a path is drawn (on a sphere with its center at point O) by the intersection point of the axis OX_3''' of the eigenrotations and the sphere. The aforementioned track describes a spherical curve lying between two horizontal circles having the shape shown in Fig. 2.19. At large value of the gyroscope rotations, the nutation angle ϑ_e takes on small values, and consequently the gyroscope motion differs slightly from a regular precession. For this reason, the motion of the gyroscope for this case is called a *pseudoregular precession*.

2.2.4 The Kovalevskaya Case of Spherical Motion of a Rigid Body

Until the end of the nineteenth century, cases of spherical motions of a rigid body, investigated by Euler and Lagrange, had been the only ones, where (2.22) and (2.23) had been completely solved. The main problem remained finding the fourth first

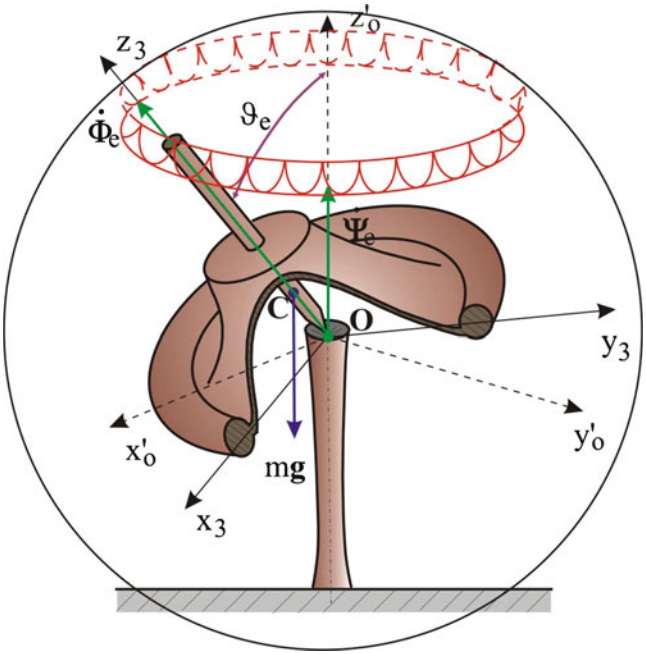

Fig. 2.19 Pseudoregular precession

integral of the Euler–Poisson equations. As was already mentioned, the three first integrals had been already determined: the trivial one $\gamma_1^2+\gamma_2^2+\gamma_3^2=1$, the energy integral $2T^2=\text{const}$, and the angular momentum integral $K_o^2=\text{const}$.

The Kovalevskaya[1] investigations showed that the fourth integral existed only for the Euler, Lagrange, and Kovalevskaya cases (i.e., for $I_{X_1'''}=I_{X_2'''}=2I_{X_3'''}$, $x_{3C}'''=0$) (Fig. 2.20).

Let us write the Euler–Poisson equations for the Kovalevskaya case, where the axes OX_1''' and OX_2''' are selected in a way that (we can always do this) the center of inertia lies on the axis OX_1''', hence $I_{X_1'''}=I_{X_2'''}=2I_{X_3'''}$, $x_{2C}'''=x_{3C}'''=0$, $x_{1C}'''=a$. Thus, we have the following system of equations:

$$2\frac{\mathrm{d}\omega_{eX_1'''}}{\mathrm{d}t}-\omega_{eX_2'''}\omega_{eX_3'''}=0, \tag{2.75a}$$

$$2\frac{\mathrm{d}\omega_{eX_2'''}}{\mathrm{d}t}+\omega_{eX_3'''}\omega_{eX_1'''}=\overline{G}\gamma_3, \tag{2.75b}$$

[1] Sofia Kovalevskaya (1850–1891), Russian mathematician.

Fig. 2.20 Kovalevskaya case

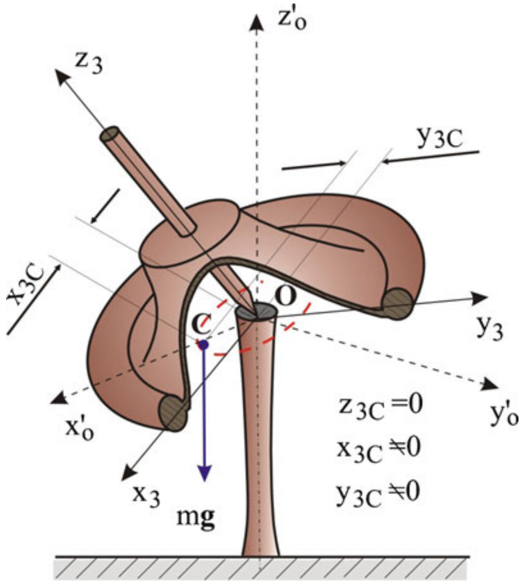

$$\frac{\mathrm{d}\omega_{eX_3'''}}{\mathrm{d}t} = -\overline{G}\gamma_2, \tag{2.75c}$$

$$\frac{\mathrm{d}\gamma_1}{\mathrm{d}t} = \omega_{eX_3'''}\gamma_2 - \omega_{eX_2'''}\gamma_3, \tag{2.76a}$$

$$\frac{\mathrm{d}\gamma_2}{\mathrm{d}t} = \omega_{eX_1'''}\gamma_3 - \omega_{eX_3'''}\gamma_1, \tag{2.76b}$$

$$\frac{\mathrm{d}\gamma_3}{\mathrm{d}t} = \omega_{eX_2'''}\gamma_1 - \omega_{eX_1'''}\gamma_2, \tag{2.76c}$$

where $\overline{G} = Ga/I_{X_3'''}$.

The preceding system of equations has three classic integrals, and we obtain them as in the Euler case. Besides the trivial integral $\gamma_1^2 + \gamma_2^2 + \gamma_3^2 = 1$, we have the energy integral

$$\frac{1}{2}\left(I_{X_1'''}\omega_{X_1'''}^2 + I_{X_2'''}\omega_{X_2'''}^2 + I_{X_3'''}\omega_{X_3'''}^2\right) + Ga\gamma_1 = \mathrm{const} \tag{2.77}$$

and the angular momentum integral

$$I_{X_3'''}\left(\omega_{X_1'''}\gamma_1 + \omega_{X_2'''}\gamma_2 + \omega_{X_3'''}\gamma_3\right) = \mathrm{const}. \tag{2.78}$$

We will determine the fourth integral in the following way. Let us introduce new variables

$$x_1^1 = \omega_{eX_1'''} + \mathrm{i}\omega_{eX_2'''}, \tag{2.79a}$$

$$x_1^2 = \gamma_1 + \mathrm{i}\gamma_2, \tag{2.79b}$$

where $\mathrm{i} = \sqrt{-1}$.

Let us multiply (2.75b) by i and sum up both sides with (2.75a). Then we obtain

$$2\dot{x}_1^1 + \mathrm{i}\omega_{eX_1'''} x_1^1 = \mathrm{i}\overline{G}\gamma_3. \tag{2.80}$$

Following similar manipulations in the first two equations of system (2.76), we find

$$\dot{x}_1^2 + \mathrm{i}\omega_{eX_1'''} x_1^2 = \mathrm{i}x_1^1\gamma_3. \tag{2.81}$$

Dividing both sides of (2.80) and (2.81) by each other, we obtain

$$2\dot{x}_1^1 x_1^1 + \mathrm{i}\omega_{eX_1'''}(x_1^1)^2 - \overline{G}\dot{x}_1^2 - \mathrm{i}\overline{G}\omega_{eX_1'''}x_1^2 = 0. \tag{2.82}$$

Following simple manipulations we obtain

$$\frac{\mathrm{d}}{\mathrm{d}t}\left((x_1^1)^2 - \overline{G}x_1^2\right) + \mathrm{i}\omega_{eX_1'''}\left((x_1^1)^2 - \overline{G}x_1^2\right) = 0, \tag{2.83a}$$

$$\frac{\mathrm{d}}{\mathrm{d}t}\ln\left((x_1^1)^2 - \overline{G}x_1^2\right) = -\mathrm{i}\omega_{eX_1'''}. \tag{2.83b}$$

The equation conjugate to (2.83b) has the following form:

$$\frac{\mathrm{d}}{\mathrm{d}t}\ln\left(\left(\overline{x_1^1}\right)^2 - \overline{G}\overline{x_1^2}\right) = \mathrm{i}\omega_{eX_1'''}. \tag{2.84}$$

Adding both sides of (2.83a) and (2.83b), we have

$$\frac{\mathrm{d}}{\mathrm{d}t}\ln\left[\left((x_1^1)^2 - \overline{G}x_1^2\right)\left(\left(\overline{x}_1^1\right)^2 - \overline{G}\overline{x_1^2}\right)\right] = 0. \tag{2.85}$$

Equation (2.85) implies that

$$\left((x_1^1)^2 - \overline{G}x_1^2\right)\left(\left(\overline{x_1^1}\right)^2 - \overline{G}\overline{x_1^2}\right) = \text{const.} \tag{2.86}$$

Going back in (2.79) to the original variables, we obtain the desired fourth first integral:

$$\left(\omega_{eX_1'''}^2 - \omega_{eX_2'''}^2 - \overline{G}\gamma_1\right)^2 + \left(2\omega_{eX_1'''}\omega_{eX_2'''} - \overline{G}\gamma_2\right)^2 = \text{const.} \tag{2.87}$$

Thus, the Kovalevskaya problem reduces to quadratures of the hyperbolic type. The character of motion of a body in the Kovalevskaya case is much more complex than in the Euler and Lagrange cases. For this reason, in these two latter cases, the general properties of motion of a rigid body were thoroughly examined, contrary to the Kovalevskaya case.

It should be emphasized that Kovalevskaya's investigations caused in the fall of the nineteenth and in the first half of the twentieth century a kind of competition among renowned mathematicians to find new solutions to the Euler–Poisson equations. As an example one can give the results of investigations of Russian mathematicians Nekrasov and Appelrot from Moscow. They gave the relations between moments of inertia and coordinates of the center of inertia of a body, at which it is possible to integrate the system of equations (2.22) and (2.23). The relations are as follows:

$$x'''_{2C} = 0, \quad x'''_{1C}\sqrt{I_{X'''_1}\left(I_{X'''_2} - I_{X'''_3}\right)} + x'''_{3C}\sqrt{I_{X'''_3}\left(I_{X'''_2} - I_{X'''_3}\right)} = 0.$$

For several decades, many outstanding scientists struggled with finding the fourth integral for another more general cases since (as was already mentioned) this would allow for the integration of the basic system of (2.22) and (2.23) by means of quadratures.

However, presently, this problem can be considered as historic since modern computers allow one to easily solve a full system of equations of spherical motion of any rigid body, with arbitrarily acting external forces. For this reason, the problem of determining the fourth integral has been out of date for a long time, but it remains open.

2.2.5 *Essence of Gyroscopic Effect*

For many centuries the lack of constraints maintaining the pivot point of a humming top at a fixed position relative to the base has blocked the practical application of the humming top.

The humming top maintains the orientation of the main axis *AA* in space only on a base with no angular movements (Fig. 2.21). If the base is inclined at the angle χ (Fig. 2.22), the humming top goes down under the action of the gravitational force $mg \sin \chi$.

The Cardan suspension (Foucault – 1852) allowed for the transformation of a humming top into a compact, axially symmetric rotor spinning freely about the so-called main axis (also called an eigenaxis) *AA* (Fig. 2.23) in an internal frame (ring). The internal frame was mounted by means of two bearings located in the *BB* axis of the external frame [9, 10].

Such a suspension provided to the rotor, along with the internal frame, makes it possible to rotate about the *BB* axis. An external frame was also mounted by means

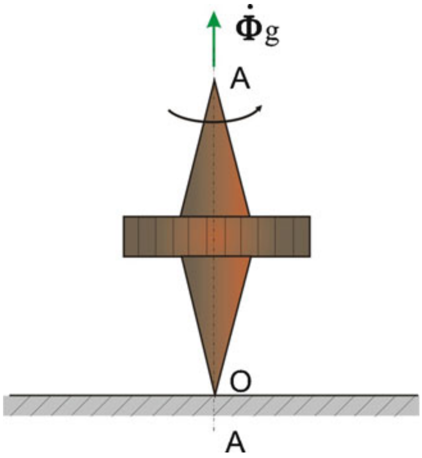

Fig. 2.21 Humming top on a horizontal base

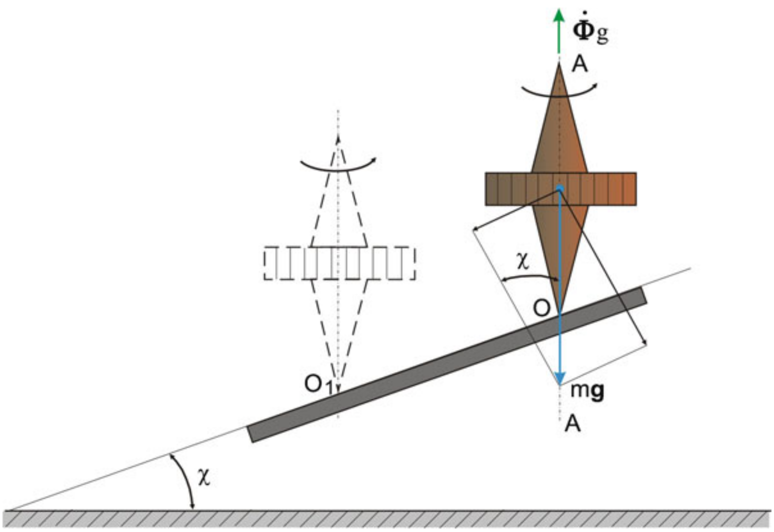

Fig. 2.22 Humming top on an inclined base

of two bearings, located on the CC axis, on the gyroscope base. In this way, the rotor, along with the internal and external frames, was given freedom of rotation about the external axis CC of suspension. Moreover, contrary to the case of the humming top, constraints imposed on support point O do not allow for displacement relative to the base.

Finally, a *gyroscope, in the technical sense, is a device in the form of a fast spinning rotor that rotates about an axis of symmetry and is suspended in a suspension (e.g., proposed by Foucault) and ensures free angular deviations relative to the base.*

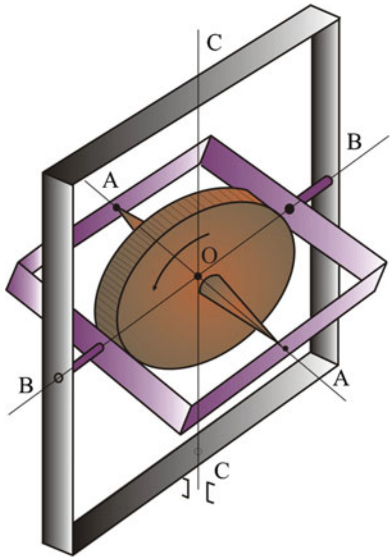

Fig. 2.23 Gyroscope in Cardan suspension

The gyroscopic effect of a fast spinning body relies on opposing any changes to its position in the space. For many centuries, the amazing phenomenon of the gyroscopic effect has seemed, to many observers, to contradict the fundamental laws of mechanics of the motion of bodies. We can observe these laws in the case of the effect of a force on the external frame of a gyroscope that attempts to turn the rotor about the *CC* axis and consequently move the main axis *AA* out of its initial position.

The external frame remains fixed, whereas the rotor with an internal frame starts to rotate about the *BB* axis. This anomaly in gyroscope motion can be explained by the fact that as the gyroscope axis changes its orientation, the Coriolis force occurs.

Let us consider, in more detail, the generation of the Coriolis force at the fast spinning gyroscope rotor about the axis OX_1''' at angular velocity $\boldsymbol{\omega}_o$ (Fig. 2.24) and simultaneously rotating about the axis OX_3''' at angular velocity $\boldsymbol{\omega}_1$. Thus in this case we are dealing with a compound motion of the rotor. Each point of the rotor participates in relative motion (rotational motion around the gyroscope axis) and in the drift motion (rotational motion about the axis OX_3'''). Then, the Coriolis acceleration will appear as a result of the drift velocity change in relative motion and the relative velocity change in drift motion.

Taking into account the fact that at an arbitrary instant of time, each material point n_i of the gyroscope rotor, distant from the axis OX_1''' at ρ_i, has a relative velocity $V_i = \omega_o \rho_i$ and angular velocity of drift ω_1 about the axis OX_3''', and its Coriolis acceleration reads

$$a_{ci} = 2\omega_o \rho_i \omega_1 \sin \Phi_i . \tag{2.88}$$

To make a material point of mass m_i accelerate with the above acceleration (2.89), one needs to apply an external force to it:

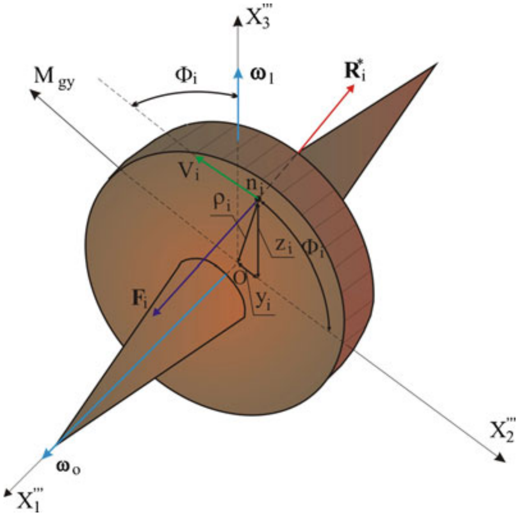

Fig. 2.24 Generation of gyroscopic moment

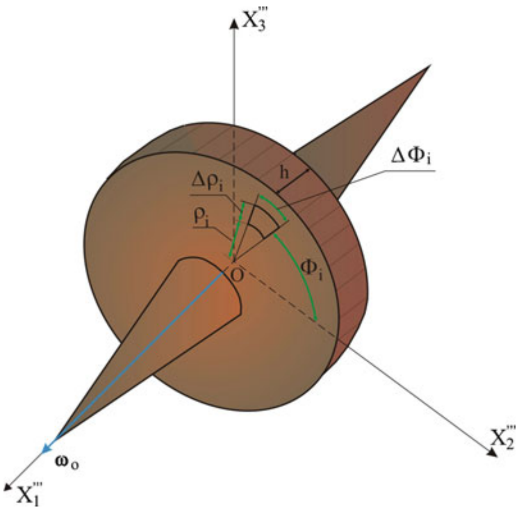

Fig. 2.25 Determining a gyroscope's mass

$$F_i = m_i a_{ci}. \tag{2.89}$$

Assuming, for the sake of simplicity, that the gyroscope rotor is disk-shaped and expressing the mass of the material point of the rotor as a product of volume and density d_r we obtain

$$m_i = d_r \Delta\rho_i \rho_i \Delta\Phi_i h, \tag{2.90}$$

where h denotes the width of the rotor disk. Substituting (2.88) and (2.90) into (2.89), we find the expression for an elemental Coriolis force (Figs. 2.24, 2.25):

$$F_i = 2 d_r \omega_0 \omega_1 h \rho_i^2 \Delta\rho_i \sin\Phi_i \Delta\Phi_i. \tag{2.91}$$

The inertial force $\boldsymbol{R}_i^*$ (Fig. 2.24), whose norm equals the norm of $\mathbf{F}_i$ and the opposite orientation, will oppose the Coriolis force (2.91). This force generates resistance torques relative to the two axes OX_2''' and OX_3''' of the form

$$M_{gx_2^i} = -R_i^* x_3^i = R_i^* \rho_i \sin \Phi_i , \tag{2.92}$$

$$M_{gx_3^i} = -R_i^* x_2^i = R_i^* \rho_i \cos \Phi_i . \tag{2.93}$$

Substituting $R_i^* = -F_i$ from (2.91), we obtain

$$M_{gx_2^i} = 2d_r \omega_0 \omega h \rho_i^3 \Delta\rho_i \sin^2\Phi_i \,\Delta\Phi_i , \tag{2.94}$$

$$M_{gx_3^i} = 2d_r \omega_0 \omega h \rho_i^3 \Delta\rho_i \sin \Phi_i \cos \Phi_i \,\Delta\Phi_i . \tag{2.95}$$

The sum of the inertial moments values (2.94) and (2.95) for the whole rotor is as follows:

$$M_{gX_2} = 2d_r \omega_o \omega_1 h \int\limits_0^R \rho^3 \mathrm{d}\rho \int\limits_0^{2\pi} \sin^2\Phi \mathrm{d}\Phi, \tag{2.96}$$

$$M_{gX_3} = 2d_r \omega_0 \omega_1 h \int\limits_0^R \rho^3 \mathrm{d}\rho \int\limits_0^{2\pi} \sin\Phi \cos\Phi \mathrm{d}\Phi, \tag{2.97}$$

where R is the radius of the gyroscope rotor.

Evaluating the integrals in (2.96) and (2.97) we obtain

$$M_{gX_2} = I_{go} \omega_o \omega_1 , \quad M_{gX_3} = 0, \tag{2.98}$$

where $I_{go} = d_r \pi R^2 h \frac{R^2}{2} = m \frac{R^2}{2}$ is the moment of inertia of the rotor relative to the main axis OX_1'''.

It follows from the preceding considerations that if the external torque M_e about the axis OX_3''' is applied to a fast spinning rotor about the axis OX_1''', then the gyroscopic torque M_{gX_2} arises about the axis OX_2'''. In Fig. 2.24 one can observe that the gyroscopic moment attempts to rotate the rotor about the axis OX_2''' in such a way that the axis of its forced rotation OX_3''' will coincide with the main axis OX_1''' of the gyroscope in the shortest distance. The aforementioned operation of the gyroscopic moment will occur during the forced rotation of the rotor about an arbitrary axis that is not the main axis of the gyroscope.

Generally, one can apply the Zhukovski principle to determine the orientation of the gyroscopic moment $\mathbf{M}_\Gamma$, which is equal to

$$\mathbf{M}_\Gamma = I_{go} \boldsymbol{\omega}_o \times \boldsymbol{\omega}_1 , \tag{2.99}$$

where $\boldsymbol{\omega}_o$ is the angular velocity of eigenrotations of a gyroscope and $\boldsymbol{\omega}_1$ is the angular velocity of the forced rotation.

The principle states that making the rotor, which spins at the angular velocity $\boldsymbol{\omega}_o$ about the main axis AA (Fig. 2.23), rotate at the angular velocity $\boldsymbol{\omega}_1$ about any axis of those remaining (BB or CC) perpendicular to AA, a moment arises whose vector $\mathbf{M}_\Gamma$ is perpendicular to vectors $\boldsymbol{\omega}_o$ and $\boldsymbol{\omega}_1$ and indicates the direction in which the coincidence of vector $\boldsymbol{\omega}_o$ with $\boldsymbol{\omega}_1$ is performed on the shortest path counterclockwise.

Generally, one can state that the gyroscopic moment is a property of a gyroscope that is used to oppose the external torques attempting to change the position of its main axis in space. It is always generated in cases where a rotating body is attached to a movable base.

The law of precession, stated by *Foucault*, is as follows [5, 11, 12]:

As a result of the action of the external moment $\mathbf{M_o}$ exerted on a gyroscopic moment, the angular velocity vector of eigenrotations $\boldsymbol{\omega}_o$ and vector $\boldsymbol{\omega}_1$ obey the following formula

$$\omega_1 = \frac{M_o}{I_{go}\omega_o}. \tag{2.100}$$

It follows from (2.100) that the angular velocity ω_o of precession of a gyroscope is proportional to the value of the moment M_o of external forces. Thus, if there is no acting moment of external forces, then there is no precession motion of a gyroscope. The position of the gyroscope in such a case will remain unchanged (and thus stable) in space. Therefore, eliminating the influence of moments of external forces on a gyroscope, by putting it in Cardan rings (Fig. 2.23), the main axis will preserve its initial position independently of displacements, velocities, and accelerations of the base. The aforementioned property of the gyroscope has found application in various navigational instruments.

References

1. G.K. Suslov, *Theoretical Mechanics* (GOSTEKHIZDAT, Moscow/Leningrad, 1946), in Russian
2. J. Awrejcewicz, *Classical Mechanics: Kinematics and Statics* (Springer, Berlin, 2012)
3. J. Awrejcewicz, *Classical Mechanics: Dynamics* (Springer, Berlin, 2012)
4. L.G. Loytsyanskiy, A.I. Lurie, *Lectures on Theoretical Mecahanics. Part 2. Dynamics* (OGIZ, Leningrad, 1948), in Russian
5. V.A. Pavlov, *Aviational Giroscopic Devices* (GOSIZDAT of the Russian Defence Industry, Moscow, 1954), in Russian
6. V.N. Koshlyakov, *Problems of Solid Body Dynamics and Applied Theory of Gyroscopes* (Nauka, Moscow, 1985), in Russian
7. A.M. Lestev, *Nonlinear Gyroscopic Systems* (LGU, Leningrad, 1983), in Russian
8. V.Ph. Zhuravlev, D.M. Klimov, *Hemispherical Resonator Gyro* (Nauka, Moscow, 1985), in Russian.
9. J.B. Scarborough, *The Gyroscope: Theory and Application* (Interscience, New York, 1958)
10. A.Yu. Ishlinskii, *Mechanics of Gyroscopic Systems*. (English translation of Russian edition) (Oldbourne, London, 1965)
11. M.A. Pavlovskiy, T.B. Putiaga, *Theoretical Mechanics* (Vyshaya Shkola, Kiev, 1985), in Russian
12. M.A. Pavlovskiy, *Theory of the Gyroscope* (Vyshaya Shkola, Kiev, 1985), in Russian

http://www.springer.com/978-1-4614-3977-6

Classical Mechanics
Applied Mechanics and Mechatronics
Awrejcewicz, J.; Koruba, Z.
2012, XXI, 250 p., Hardcover
ISBN: 978-1-4614-3977-6